

# Micromorphic media

Samuel Forest

MINES ParisTech, Centre des matériaux, CNRS UMR 7633

BP 87, 91003 Evry, France

`samuel.forest@mines-paristech.fr`

**Abstract** The elastoviscoplasticity theory of micromorphic media at finite deformation is presented in this chapter. Micromechanical considerations are then put forward to motivate the existence of the microdeformation degrees of freedom in the case of composite materials. Mixtures of micromorphic media are finally considered with a view to homogenising the size-dependent properties of metal polycrystals.

## 1 Introduction

### 1.1 Scope of this chapter

A classification of generalised mechanical continuum theories is proposed in Fig. 1. The present chapter is limited to continuum media fulfilling the principle of local action, meaning that the mechanical state at a material point  $\underline{\mathbf{X}}$  depends on variables defined at this point only (Truesdell and Toupin, 1960; Truesdell and Noll, 1965). The classical Cauchy continuum is called *simple material* because its response at material point  $\underline{\mathbf{X}}$  to deformations homogeneous in a neighborhood of  $\underline{\mathbf{X}}$  determines uniquely its response to every deformation at  $\underline{\mathbf{X}}$ . In *higher grade* materials, homogeneous deformations are not sufficient to characterise the material behaviour because they are sensitive to higher gradients of the displacement field. Mindlin formulated for instance the theories that include the second and third gradients of the displacement field (Mindlin, 1965). The gradient effect may be limited to the plastic part of deformation which leads to strain gradient plasticity models (Aifantis, 1984; Forest and Bertram, 2011) or, more generally, theories that include the gradient of some internal variables (Maugin, 1990). *Higher order* materials are characterised by additional degrees of freedom of the material points (Eringen, 1999). Directors can be attached to each material point that evolve in a different way from the material lines. Cosserat directors can rotate. In the micromorphic continuum designed by

Eringen and Mindlin (Eringen and Suhubi, 1964; Mindlin, 1964), the directors can also be distorted, so that a second order tensor is attributed to each material point. Tensors of higher order can even be introduced as proposed in Germain's general micromorphic theory (Germain, 1973).

Higher order media are sometimes called continua with *microstructure*. This name has now become misleading in the sense that even Cauchy material models can integrate some aspects of the underlying microstructure as illustrated by classical homogenisation methods used to derive the effective properties of composites. However generalised continua incorporate a feature of the microstructure which is not accounted for by standard homogenisation methods, namely their size-dependent material response. They involve intrinsic lengths directly stemming from the microstructure of the material. The micromorphic theory now arouses strong interest from the materials science and computational mechanics communities because of its regularisation power in the context of softening plasticity and damage and of its rather simple implementation in a finite element program. The number of degrees of freedom is not an obstacle any more with constantly increasing computer power.

The objective of this chapter is first to present the elastoviscoplasticity theory of micromorphic media at finite deformation. This presentation is based on the fundamental work of Eringen and on recent developments in the context of plasticity. The second part is dedicated to the motivation of higher order degrees of freedom by means of extended homogenisation methods. Finally the question of heterogeneous micromorphic media is addressed, with a view to applications in polycrystalline plasticity.

## 1.2 Notations

First, second, third, fourth and sixth order tensors are denoted by  $\underline{\underline{\underline{\underline{\underline{A}}}}}$ ,  $\underline{\underline{\underline{\underline{A}}}}$ ,  $\underline{\underline{\underline{A}}}$ ,  $\underline{\underline{A}}$  and  $\underline{\underline{\underline{\underline{\underline{A}}}}}$  respectively. Their components will be considered with respect to a Cartesian basis:

$$\underline{\underline{\underline{\underline{\underline{A}}}}} = A_i \underline{\underline{\underline{\underline{\underline{e}}}}}_i, \quad \underline{\underline{\underline{\underline{A}}}} = A_{ij} \underline{\underline{\underline{\underline{e}}}}_i \otimes \underline{\underline{\underline{\underline{e}}}}_j, \quad \underline{\underline{\underline{A}}} = \underline{\underline{\underline{A}}} = A_{ijk} \underline{\underline{\underline{e}}}_i \otimes \underline{\underline{\underline{e}}}_j \otimes \underline{\underline{\underline{e}}}_k$$

The following tensor products are defined

$$\underline{\underline{\underline{\underline{\underline{a}}}}} \otimes \underline{\underline{\underline{\underline{\underline{b}}}}} = a_i b_j \underline{\underline{\underline{\underline{\underline{e}}}}}_i \otimes \underline{\underline{\underline{\underline{\underline{e}}}}}_j, \quad \underline{\underline{\underline{\underline{A}}}} \otimes \underline{\underline{\underline{\underline{B}}}} = A_{ij} B_{kl} \underline{\underline{\underline{\underline{e}}}}_i \otimes \underline{\underline{\underline{\underline{e}}}}_j \otimes \underline{\underline{\underline{\underline{e}}}}_k \otimes \underline{\underline{\underline{\underline{e}}}}_l$$

$$\underline{\underline{\underline{\underline{A}}}} \boxtimes \underline{\underline{\underline{\underline{B}}}} = A_{ik} B_{jl} \underline{\underline{\underline{\underline{e}}}}_i \otimes \underline{\underline{\underline{\underline{e}}}}_j \otimes \underline{\underline{\underline{\underline{e}}}}_k \otimes \underline{\underline{\underline{\underline{e}}}}_l$$

The tensor simple and multiple contractions follow the next rules:

$$\underline{\underline{\underline{\underline{\underline{A}}}}} \cdot \underline{\underline{\underline{\underline{\underline{B}}}}} = A_i B_i, \quad \underline{\underline{\underline{\underline{A}}}} : \underline{\underline{\underline{\underline{B}}}} = A_{ij} B_{ij}, \quad \underline{\underline{\underline{\underline{\underline{A}}}}} \dot{\cdot} \underline{\underline{\underline{\underline{\underline{B}}}}} = A_{ijk} B_{ijk}$$

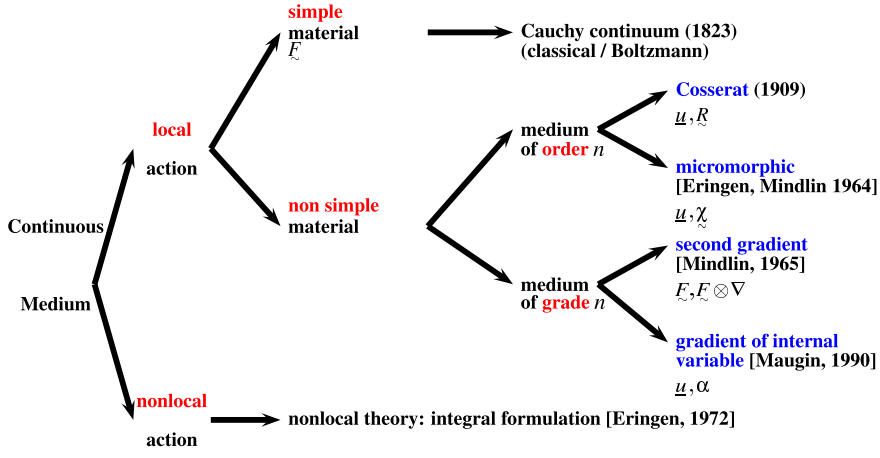


**Figure 1.** A classification of the mechanics of generalised continua.

For tensor analysis, nabla operators  $\nabla_X$  and  $\nabla_x$  are defined with respect to the reference and current configurations of the body, respectively.

$$\nabla_x = ,i \underline{e}_i = \frac{\partial}{\partial x_i} \underline{e}_i, \quad \nabla_X = ,J \underline{E}_J = \frac{\partial}{\partial X_J} \underline{E}_J$$

where  $(\underline{E}_J)_{J=1,3}$  and  $(\underline{e}_i)_{i=1,3}$  denote the corresponding Cartesian bases. The comma stands for partial derivative with respect to the corresponding coordinate. The following rules are adopted

$$\underline{u} \otimes \nabla = u_{i,j} \underline{e}_i \otimes \underline{e}_j, \quad \underline{\sigma} \cdot \nabla = \sigma_{ij,j} \underline{e}_i$$

## 2 Micromorphic continua

### 2.1 Kinematics of micromorphic media

The degrees of freedom of the theory are the displacement vector  $\underline{u}$  and the microdeformation tensor  $\underline{\chi}$ :

$$DOF := \{ \underline{u}, \underline{\chi} \}$$

The current position of the material point is given by the transformation  $\Phi$  according to  $\underline{x} = \Phi(\underline{X}) = \underline{X} + \underline{u}(\underline{X})$ . The microdeformation describes

name	number of DOF	DOF	references
Cauchy	3	$\underline{\mathbf{u}}$	Cauchy (1822)
microdilatation	4	$\underline{\mathbf{u}}, \chi$	Goodman and Cowin (1972) Steeb and Diebels (2003)
Cosserat	6	$\underline{\mathbf{u}}, \underline{\mathbf{R}}$	Kafadar and Eringen (1971)
microstretch	7	$\underline{\mathbf{u}}, \chi, \underline{\mathbf{R}}$	Eringen (1990)
microstrain	9	$\underline{\mathbf{u}}, \underline{\mathbf{C}}^\sharp$	Forest and Sievert (2006)
micromorphic	12	$\underline{\mathbf{u}}, \underline{\mathbf{\chi}}$	Eringen and Suhubi (1964) Mindlin (1964)

**Table 1.** A hierarchy of higher order continua.

the deformation of a triad of directors,  $\underline{\Xi}^i$  attached to the material point

$$\underline{\xi}^i(\underline{\mathbf{X}}) = \underline{\chi}(\underline{\mathbf{X}}) \cdot \underline{\Xi}^i \quad (1)$$

The polar decomposition of the generally incompatible microdeformation field  $\underline{\chi}(\underline{\mathbf{X}})$  is introduced

$$\underline{\chi} = \underline{\mathbf{R}}^\sharp \cdot \underline{\mathbf{U}}^\sharp \quad (2)$$

Internal constraints can be prescribed to the microdeformation. The micromorphic medium reduces to the Cosserat medium when the microdeformation is constrained to be a pure rotation:  $\underline{\chi} \equiv \underline{\mathbf{R}}^\sharp$ . The microstrain medium is obtained when  $\underline{\chi} \equiv \underline{\mathbf{U}}^\sharp$  (Forest and Sievert, 2006). Finally, the second gradient theory is retrieved when the microdeformation coincides with the deformation gradient,  $\underline{\chi} \equiv \underline{\mathbf{F}}$ . A hierarchy of higher order continua can be established by specialising the micromorphic theory and depending on the targeted material class, see Table 1.

The following kinematical quantities are then introduced:

- the velocity field  $\underline{\mathbf{v}}(\underline{\mathbf{x}}) := \underline{\dot{\mathbf{u}}}(\Phi^{-1}(\underline{\mathbf{x}}))$

- the deformation gradient  $\underline{\mathbf{F}} = \underline{\mathbf{1}} + \underline{\mathbf{u}} \otimes \nabla_X$
- the velocity gradient  $\underline{\mathbf{v}} \otimes \nabla_x = \dot{\underline{\mathbf{F}}} \cdot \underline{\mathbf{F}}^{-1}$
- the microdeformation rate  $\dot{\underline{\chi}} \cdot \underline{\chi}^{-1}$
- the Lagrangean microdeformation gradient  $\underline{\mathbf{K}} := \underline{\chi}^{-1} \cdot \underline{\chi} \otimes \nabla_X$
- the gradient of the microdeformation rate tensor

$$(\dot{\underline{\chi}} \cdot \underline{\chi}^{-1}) \otimes \nabla_x = \underline{\chi} \cdot \dot{\underline{\mathbf{K}}} : (\underline{\chi}^{-1} \boxtimes \underline{\mathbf{F}}^{-1}) \quad (3)$$

and the corresponding index notation:

$$(\dot{\chi}_{il} \chi_{lj}^{-1})_{,k} = \chi_{ip} \dot{K}_{pqr} \chi_{qj}^{-1} F_{rk}^{-1}$$

## 2.2 Principle of virtual power

The method of virtual power is used to introduce the generalised stress tensors and the field and boundary equations they must satisfy (Germain, 1973).

The modelling variables are introduced according to a first gradient theory:

$$MODEL = \{ \underline{\mathbf{v}}, \underline{\mathbf{v}} \otimes \nabla_x, \dot{\underline{\chi}} \cdot \underline{\chi}^{-1}, (\dot{\underline{\chi}} \cdot \underline{\chi}^{-1}) \otimes \nabla_x \}$$

The virtual power of internal forces of a subdomain  $\mathcal{D} \subset \mathcal{B}$  of the body is

$$\mathcal{P}^{(i)}(\underline{\mathbf{v}}^*, \dot{\underline{\chi}}^* \cdot \underline{\chi}^{*-1}) = \int_{\mathcal{D}} p^{(i)}(\underline{\mathbf{v}}^*, \dot{\underline{\chi}}^* \cdot \underline{\chi}^{*-1}) dV$$

The virtual power density of internal forces is a linear form on the fields of virtual modeling variables:

$$\begin{aligned} p^{(i)} &= \underline{\boldsymbol{\sigma}} : (\dot{\underline{\mathbf{F}}} \cdot \underline{\mathbf{F}}^{-1}) + \underline{\boldsymbol{s}} : (\dot{\underline{\mathbf{F}}} \cdot \underline{\mathbf{F}}^{-1} - \dot{\underline{\chi}} \cdot \underline{\chi}^{-1}) + \underline{\underline{\mathbf{M}}} : ((\dot{\underline{\chi}} \cdot \underline{\chi}^{-1}) \otimes \nabla_x) \\ &= \underline{\boldsymbol{\sigma}} : (\dot{\underline{\mathbf{F}}} \cdot \underline{\mathbf{F}}^{-1}) + \underline{\boldsymbol{s}} : (\underline{\chi} \cdot (\underline{\chi}^{-1} \cdot \dot{\underline{\mathbf{F}}}) \cdot \underline{\mathbf{F}}^{-1}) \\ &+ \underline{\underline{\mathbf{M}}} : (\underline{\chi} \cdot \dot{\underline{\mathbf{K}}} : (\underline{\chi}^{-1} \boxtimes \underline{\mathbf{F}}^{-1})) \end{aligned} \quad (4)$$

where the relative deformation rate  $\dot{\underline{\mathbf{F}}} \cdot \underline{\mathbf{F}}^{-1} - \dot{\underline{\chi}} \cdot \underline{\chi}^{-1}$  is introduced and expressed in terms of the rate of the relative deformation  $\underline{\chi}^{-1} \cdot \dot{\underline{\mathbf{F}}}$ . The virtual power density of internal forces is invariant with respect to virtual rigid body motions so that  $\underline{\boldsymbol{\sigma}}$  must be symmetric. The generalised stress tensors conjugate to the velocity gradient, the relative deformation rate and the gradient of the microdeformation rate are the simple stress tensor  $\underline{\boldsymbol{\sigma}}$ , the relative stress tensor  $\underline{\boldsymbol{s}}$  and the double stress  $\underline{\underline{\mathbf{M}}}$ .

The Gauss theorem is then applied to the power of internal forces

$$\begin{aligned} \int_{\mathcal{D}} p^{(i)} dV &= \int_{\partial\mathcal{D}} \underline{\mathbf{v}}^* \cdot (\underline{\boldsymbol{\sigma}} + \underline{\boldsymbol{s}}) \cdot \underline{\mathbf{n}} dS + \int_{\partial\mathcal{D}} (\dot{\underline{\boldsymbol{\chi}}}^* \cdot \underline{\boldsymbol{\chi}}^{*-1}) : \underline{\underline{\mathbf{M}}} \cdot \underline{\mathbf{n}} dS \\ &- \int_{\mathcal{D}} \underline{\mathbf{v}}^* \cdot (\underline{\boldsymbol{\sigma}} + \underline{\boldsymbol{s}}) \cdot \nabla_x dV - \int_{\mathcal{D}} (\dot{\underline{\boldsymbol{\chi}}}^* \cdot \underline{\boldsymbol{\chi}}^{*-1}) : (\underline{\underline{\mathbf{M}}} \cdot \nabla_x + \underline{\boldsymbol{s}}) dV \end{aligned}$$

The form of the previous boundary integral dictates the form of the power of contact forces acting on the boundary  $\partial\mathcal{D}$  of the subdomain  $\mathcal{D} \subset \mathcal{B}$

$$\mathcal{P}^{(c)}(\underline{\mathbf{v}}^*, \dot{\underline{\boldsymbol{\chi}}}^* \cdot \underline{\boldsymbol{\chi}}^{*-1}) = \int_{\partial\mathcal{D}} p^{(c)}(\underline{\mathbf{v}}^*, \dot{\underline{\boldsymbol{\chi}}}^* \cdot \underline{\boldsymbol{\chi}}^{*-1}) dV$$

$$p^{(c)}(\underline{\mathbf{v}}^*, \dot{\underline{\boldsymbol{\chi}}}^* \cdot \underline{\boldsymbol{\chi}}^{*-1}) = \underline{\mathbf{t}} \cdot \underline{\mathbf{v}}^* + \underline{\mathbf{m}} : (\dot{\underline{\boldsymbol{\chi}}}^* \cdot \underline{\boldsymbol{\chi}}^{*-1})$$

where the simple traction  $\underline{\mathbf{t}}$  and double traction  $\underline{\mathbf{m}}$  are introduced.

The power of forces acting at a distance is defined as

$$\mathcal{P}^{(e)}(\underline{\mathbf{v}}^*, \dot{\underline{\boldsymbol{\chi}}}^* \cdot \underline{\boldsymbol{\chi}}^{*-1}) = \int_{\mathcal{D}} p^{(e)}(\underline{\mathbf{v}}^*, \dot{\underline{\boldsymbol{\chi}}}^* \cdot \underline{\boldsymbol{\chi}}^{*-1}) dV$$

$$p^{(e)}(\underline{\mathbf{v}}^*, \dot{\underline{\boldsymbol{\chi}}}^* \cdot \underline{\boldsymbol{\chi}}^{*-1}) = \underline{\mathbf{f}} \cdot \underline{\mathbf{v}}^* + \underline{\mathbf{p}} : (\dot{\underline{\boldsymbol{\chi}}}^* \cdot \underline{\boldsymbol{\chi}}^{*-1})$$

including simple body forces  $\underline{\mathbf{f}}$  and double body forces  $\underline{\mathbf{p}}$ . More general double and triple volume forces could also be incorporated according to Germain (1973).

The principle of virtual power is now stated in the static case,

$$\forall \underline{\mathbf{v}}^*, \forall \dot{\underline{\boldsymbol{\chi}}}^*, \forall \mathcal{D} \subset \mathcal{B}, \mathcal{P}^{(i)}(\underline{\mathbf{v}}^*, \dot{\underline{\boldsymbol{\chi}}}^* \cdot \underline{\boldsymbol{\chi}}^{*-1}) = \mathcal{P}^{(c)}(\underline{\mathbf{v}}^*, \dot{\underline{\boldsymbol{\chi}}}^* \cdot \underline{\boldsymbol{\chi}}^{*-1}) + \mathcal{P}^{(e)}(\underline{\mathbf{v}}^*, \dot{\underline{\boldsymbol{\chi}}}^* \cdot \underline{\boldsymbol{\chi}}^{*-1})$$

This variational formulation leads to

$$\begin{aligned} &\int_{\partial\mathcal{D}} \underline{\mathbf{v}}^* \cdot (\underline{\boldsymbol{\sigma}} + \underline{\boldsymbol{s}}) \cdot \underline{\mathbf{n}} dS + \int_{\partial\mathcal{D}} (\dot{\underline{\boldsymbol{\chi}}}^* \cdot \underline{\boldsymbol{\chi}}^{*-1}) : \underline{\underline{\mathbf{M}}} \cdot \underline{\mathbf{n}} dS \\ &- \int_{\mathcal{D}} \underline{\mathbf{v}}^* \cdot ((\underline{\boldsymbol{\sigma}} + \underline{\boldsymbol{s}}) \cdot \nabla_x + \underline{\mathbf{f}}) dV - \int_{\mathcal{D}} (\dot{\underline{\boldsymbol{\chi}}}^* \cdot \underline{\boldsymbol{\chi}}^{*-1}) : (\underline{\underline{\mathbf{M}}} \cdot \nabla_x + \underline{\boldsymbol{s}} + \underline{\mathbf{p}}) dV = 0 \end{aligned}$$

which delivers the field equations of the problem (Kirchner and Steinmann, 2005; Lazar and Maugin, 2007; Hirschberger et al., 2007):

- balance of momentum equation (static case)

$$(\underline{\boldsymbol{\sigma}} + \underline{\boldsymbol{s}}) \cdot \nabla_x + \underline{\mathbf{f}} = 0, \quad \forall \underline{\mathbf{x}} \in \mathcal{B} \quad (5)$$

- balance of generalized moment of momentum equation (static case)

$$\underline{\underline{M}} \cdot \nabla_x + \underline{s} + \underline{p} = 0, \quad \forall \underline{x} \in \mathcal{B} \quad (6)$$

- boundary conditions

$$(\underline{\sigma} + \underline{s}) \cdot \underline{n} = \underline{t}, \quad \forall \underline{x} \in \partial \mathcal{B} \quad (7)$$

$$\underline{\underline{M}} \cdot \underline{n} = \underline{m}, \quad \forall \underline{x} \in \partial \mathcal{B} \quad (8)$$

### 2.3 Elastoviscoplasticity of micromorphic media

#### Elastic–plastic decomposition of the generalised strain measures

According to Eringen (1999), the following Lagrangean strain measures are adopted:

$$STRAIN = \{\underline{\underline{C}} := \underline{\underline{F}}^T \cdot \underline{\underline{F}}, \quad \underline{\underline{\gamma}} := \underline{\underline{\chi}}^{-1} \cdot \underline{\underline{F}}, \quad \underline{\underline{K}} := \underline{\underline{\chi}}^{-1} \cdot (\underline{\underline{\chi}} \otimes \nabla_x)\}$$

i.e. the Cauchy–Green strain tensor, the relative deformation and the microdeformation gradient.

In the presence of plastic deformation, the question arises of splitting the previous Lagrangean strain measures into elastic and plastic contributions. Following Mandel (1973), a multiplicative decomposition of the deformation gradient is postulated:

$$\underline{\underline{F}} = \underline{\underline{F}}^e \cdot \underline{\underline{F}}^p = \underline{\underline{R}}^e \cdot \underline{\underline{U}}^e \cdot \underline{\underline{F}}^p \quad (9)$$

which defines an intermediate local configuration at each material point, see Fig. 2. Uniqueness of the decomposition requires the suitable definition of directors. Such directors are available in any micromorphic theory.

A multiplicative decomposition of the microdeformation is also considered:

$$\underline{\underline{\chi}} = \underline{\underline{\chi}}^e \cdot \underline{\underline{\chi}}^p = \underline{\underline{R}}^{e\sharp} \cdot \underline{\underline{U}}^{e\sharp} \cdot \underline{\underline{\chi}}^p \quad (10)$$

according to Forest and Sievert (2003, 2006). The uniqueness of the decomposition also requires the suitable definition of directors. As an example, lattice directions in a single crystal are physically relevant directors for an elastoviscoplasticity micromorphic theory, see (Aslan et al., 2011). Finally, a partition rule must also be proposed for the third strain measure, namely the microdeformation gradient. Sansour (1998a,b) introduced an additive decomposition of curvature:

$$\underline{\underline{K}} = \underline{\underline{K}}^e + \underline{\underline{K}}^p \quad (11)$$

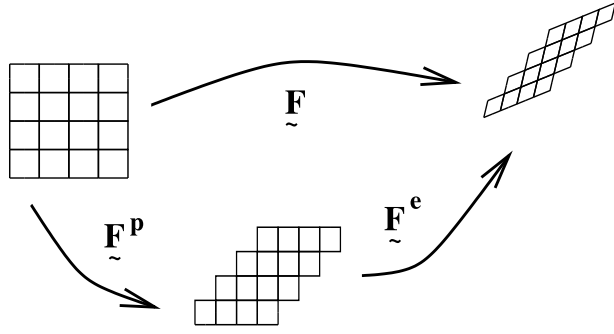


**Figure 2.** Multiplicative decomposition of the deformation gradient.

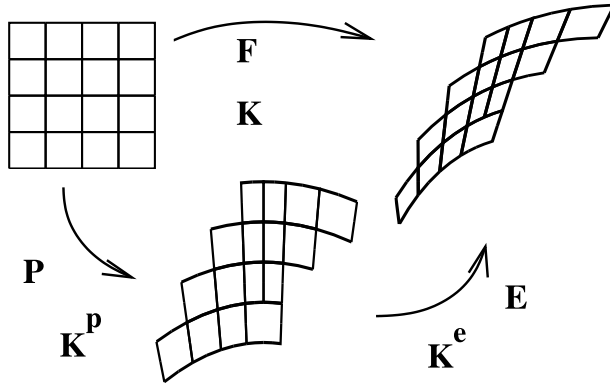


**Figure 3.** Definition of an intermediate local configuration for micromorphic elastoplasticity.

A quasi-additive decomposition was proposed by Forest and Sievert (2003) with the objective of defining an intermediate local configuration for which all generalised stress tensor are simultaneously released, as it will become apparent in the next section:

$$\underline{\underline{K}} = \underline{\underline{\chi}}^{p-1} \cdot \underline{\underline{K}}^e : (\underline{\underline{\chi}}^p \boxtimes \underline{\underline{F}}^p) + \underline{\underline{K}}^p \quad (12)$$

see Fig. 3.

### Constitutive equations

The continuum thermodynamic formulation is essentially unchanged in the presence of additional degrees of freedom provided that all functionals are properly extended to the new sets of variables. The local equation of energy balance is written in its usual form:

$$\rho \dot{\epsilon} = p^{(i)} - \underline{\mathbf{q}} \cdot \nabla + r$$

where  $\epsilon$  is the specific internal energy density, and  $p^{(i)}$  is the power density of internal forces according to Eq. (4). The heat flux vector is  $\underline{\mathbf{q}}$  and  $r$  is a heat source term. The local form of the second principle of thermodynamics is written as

$$\rho \dot{\eta} + \left( \frac{\underline{\mathbf{q}}}{T} \right) \cdot \nabla - \frac{r}{T} \geq 0$$

where  $\eta$  is the specific entropy density. Introducing the Helmholtz free energy function  $\psi$ , the second law becomes

$$p^{(i)} - \rho \dot{\Psi} - \eta \dot{T} - \frac{\underline{\mathbf{q}}}{T} \cdot (\nabla T) \geq 0$$

The state variables of the elastoviscoplastic micromorphic material are all the elastic strain measures and a set of internal variables  $q$ . The free energy density is a function of the state variables:

$$\Psi(\underline{\mathbf{C}}^e := \underline{\mathbf{F}}^{eT} \cdot \underline{\mathbf{F}}^e, \quad \underline{\mathbf{\Upsilon}}^e := \underline{\mathbf{\chi}}^{e-1} \cdot \underline{\mathbf{F}}^e, \quad \underline{\mathbf{K}}^e, \quad q)$$

The exploitation of the entropy inequality leads to the definition of the hyperelastic state laws in the form:

$$\begin{aligned} \underline{\boldsymbol{\sigma}} &= 2\underline{\mathbf{F}}^e \cdot \rho \frac{\partial \Psi}{\partial \underline{\mathbf{C}}^e} \cdot \underline{\mathbf{F}}^{eT}, \quad \underline{\mathbf{s}} = \underline{\mathbf{R}}^{e\#} \cdot \underline{\mathbf{U}}^{e\#-1} \cdot \rho \frac{\partial \Psi}{\partial \underline{\mathbf{\Upsilon}}^e} \cdot \underline{\mathbf{F}}^{eT} \\ \underline{\underline{\mathbf{M}}} &= \underline{\mathbf{\chi}}^{-T} \cdot \rho \frac{\partial \Psi}{\partial \underline{\mathbf{K}}^e} : (\underline{\mathbf{\chi}}^T \boxtimes \underline{\mathbf{F}}^T) \end{aligned} \quad (13)$$

while the entropy density is still given by  $\eta = -\frac{\partial \Psi}{\partial T}$ . The thermodynamic force associated with the internal variable  $q$  is

$$R = -\rho \frac{\partial \Psi}{\partial q}$$

The hyperelasticity law (13) for the double stress tensor was derived for the additive decomposition (11). The quasi-additive decomposition (12) leads to an hyperelastic constitutive equation for the conjugate stress  $\underline{\underline{\mathbf{M}}}$  in the

current configuration, that has also the same form as for pure hyperelastic behaviour. One finds:

$$\underline{\underline{\mathbf{M}}} = \underline{\underline{\chi}}^{e-T} \cdot \rho \frac{\partial \Psi}{\partial \underline{\underline{\mathbf{K}}}^e} : (\underline{\underline{\chi}}^{eT} \boxtimes \underline{\underline{\mathbf{F}}}^{eT}) \quad (14)$$

The residual intrinsic dissipation is

$$D = \underline{\underline{\Sigma}} : (\dot{\underline{\underline{\mathbf{F}}}}^p \cdot \underline{\underline{\mathbf{F}}}^{p-1}) + \underline{\underline{\mathcal{S}}} : (\dot{\underline{\underline{\chi}}}^p \cdot \underline{\underline{\chi}}^{p-1}) + \underline{\underline{\mathcal{S}}}_0 : \dot{\underline{\underline{\mathbf{K}}}}^p + R\dot{q} \geq 0$$

where generalised Mandel stress tensors have been defined

$$\underline{\underline{\Sigma}} = \underline{\underline{\mathbf{F}}}^{eT} \cdot (\underline{\underline{\sigma}} + \underline{\underline{s}}) \cdot \underline{\underline{\mathbf{F}}}^{e-T}, \quad \underline{\underline{\mathcal{S}}} = -\underline{\underline{\mathcal{U}}}^{e\sharp} \cdot \underline{\underline{\mathbf{R}}}^{e\sharp T} \cdot \underline{\underline{s}} \cdot \underline{\underline{\mathbf{R}}}^{e\sharp} \cdot \underline{\underline{\mathcal{U}}}^{e\sharp-1}$$

$$\underline{\underline{\mathcal{M}}} = \underline{\underline{\chi}}^T \cdot \underline{\underline{\mathcal{S}}} : (\underline{\underline{\chi}}^{-T} \boxtimes \underline{\underline{\mathbf{F}}}^{-T})$$

At this stage, one may define a dissipation potential, function of the Mandel stress tensors, from which the viscoplastic flow rule and the evolution equations for the internal variables are derived

$$\Omega(\underline{\underline{\Sigma}}, \underline{\underline{\mathcal{S}}}, \underline{\underline{\mathcal{S}}}_0)$$

$$\dot{\underline{\underline{\mathbf{F}}}}^p \cdot \underline{\underline{\mathbf{F}}}^{p-1} = \frac{\partial \Omega}{\partial \underline{\underline{\Sigma}}}, \quad \dot{\underline{\underline{\chi}}}^p \cdot \underline{\underline{\chi}}^{p-1} = \frac{\partial \Omega}{\partial \underline{\underline{\mathcal{S}}}}, \quad \dot{\underline{\underline{\mathbf{K}}}}^p = \frac{\partial \Omega}{\partial \underline{\underline{\mathcal{M}}}}, \quad \dot{q} = \frac{\partial \Omega}{\partial R}$$

The convexity of the dissipation potential with respect to its arguments ensures the positivity of the dissipation rate at each instant.

Explicit constitutive equations can be found in (Forest and Sievert, 2003; Grammenoudis and Tsakmakis, 2009; Grammenoudis et al., 2009; Regueiro, 2010; Sansour et al., 2010). Examples of application of elastoplastic micromorphic media can be found in (Dillard et al., 2006) for plasticity and failure of metallic foams.

### 3 From a heterogeneous Cauchy material to a homogeneous equivalent micromorphic medium

Two major obstacles to the use of such sophisticated continuum models are the physical interpretation of the additional degrees of freedom and the identification of the numerous additional material parameters arising in the constitutive functions of the model. Generalised continua are very often referred to as *media with microstructure* without giving precisely the link between the phenomenological constitutive equations and the detailed microstructure of the material. The mechanics of heterogeneous materials and

homogenisation methods are widely used to derive the effective properties of classical Cauchy materials based on the description of a representative volume element. Extension of these methods to generalised continua would establish clear definitions of the macroscopic degrees of freedom and provide a systematic way of deriving additional macroscopic materials parameters. Homogenization techniques already exist to construct 1D Cosserat beam models and 2D Mindlin plate models (Altenbach et al., 2010). In the case of 3D generalised continua, it has been proposed in (Gologanu et al., 1997; Forest, 1998, 1999) to construct an effective generalised continuum model starting from a heterogeneous classical Cauchy material by means of extended homogenisation methods.

The present part concentrates on the construction of an overall strain gradient or micromorphic continuum from a microscopic heterogeneous Cauchy material. Such a generalised continuum approach is necessary when significantly high strain gradients develop at the macroscopic scale, more precisely, when the wave length of variation of the macroscopic fields is not sufficiently large compared to the size of the heterogeneities.

For that purpose, quadratic boundary conditions to be applied on a RVE were first proposed in (Gologanu et al., 1997; Forest and Sab, 1998) to construct an effective second gradient and Cosserat overall continuum, respectively. They represent extensions of the classical affine conditions used in classical homogenisation theory (Besson et al., 2009). They were used to identify higher order stiffness, typically bending stiffnesses, that are necessary to account for fiber size effect in composites under significant macroscopic strain gradients, in (Ostoja-Starzewski et al., 1999; Bouyge et al., 2001, 2002; Sansalone et al., 2006; Chen et al., 2009; Anthoine, 2010). Cosserat approaches are particularly well-suited to describe the effective behaviour of civil engineering and granular materials, as shown in (Trovalusci and Masiani, 2003; Goddard, 2008; Salerno and de Felice, 2009; Besdo, 2010).

Such higher order homogenisation schemes have been used in so-called  $FE^2$  methods for which the constitutive model at each material of a computed structure is replaced by the resolution of a boundary value problem on the unit cell of the underlying heterogeneous material. The method is computationally very expensive but makes it possible to address nonlinear problems without writing explicit constitutive laws in the generalised continuum model. In (Feyel, 2003), the Cosserat model is used at the macro-level to represent a fiber matrix composite and the quadratic and cubic boundary conditions proposed by Forest and Sab (1998) are applied to each unit cell. In the references (Geers et al., 2001; Kouznetsova et al., 2002, 2004), the macroscopic medium is regarded as a strain gradient continuum so that

quadratic boundary conditions are sufficient. More recently, a micromorphic overall continuum was considered in (Forest, 2002; Jänicke et al., 2009; Jänicke and Diebels, 2009) which represents currently the most general extension of classical homogenisation models.

In most cases however, the proposed extended homogenisation procedures remain heuristic and several questions are still pending: existence of a representative volume element in the presence of non-homogeneous boundary conditions, properties of the local fluctuation field in the case of a polynomial macro-field, as recently addressed by (Yuan et al., 2008; Forest and Trinh, 2011), and the contribution of this fluctuation to the extended Hill-Mandel condition.

The micromorphic theory is used in this part in the small deformation context for simplicity. Capital letters will denote variables attached to the microscopic homogenized model, whereas small letters will characterize the microstructure level. The representative volume element of the material (RVE), a simple unit cell in the periodic case, is made of a heterogeneous Cauchy continuum characteristic of a composite material. The local coordinate in the unit cell  $V(\underline{\mathbf{X}})$  with centre  $\underline{\mathbf{X}}$ , is denoted by  $\underline{\mathbf{x}}$ .

The degrees of freedom represented by the generally non-symmetric second order tensor field,  $\underline{\underline{\chi}}(\underline{\mathbf{X}})$ , are introduced in addition to the displacement degrees of freedom,  $\underline{\underline{\mathbf{U}}}(\underline{\mathbf{X}})$ . It is assumed that the development of microdeformation gradient

$$\underline{\underline{\mathbf{K}}}(\underline{\mathbf{X}}) = \underline{\underline{\chi}}(\underline{\mathbf{X}}) \otimes \nabla_{\underline{\mathbf{x}}} \quad (15)$$

is associated with internal work and energy storage. There is also an energetic price to pay for the microdeformation to depart from the macrodeformation, characterised by the relative deformation measure:

$$\underline{\underline{\mathbf{e}}}(\underline{\mathbf{X}}) = \underline{\underline{\mathbf{U}}}(\underline{\mathbf{X}}) \otimes \nabla_{\underline{\mathbf{x}}} - \underline{\underline{\chi}}(\underline{\mathbf{X}}) \quad (16)$$

The micromorphic model encompasses the strain gradient theory as a limit case if the internal constraint

$$\underline{\underline{\chi}} \equiv \underline{\underline{\mathbf{U}}} \otimes \nabla_{\underline{\mathbf{x}}} \iff \underline{\underline{\mathbf{e}}} \equiv 0 \quad (17)$$

is enforced (Forest, 2009).

### 3.1 Definition of the micromorphic degrees of freedom

A kinematic view of the micromorphic model has been proposed by Germain (1973), that we rephrase here. *In a theory which takes microstructure into account, from the macroscopic point of view of continuum mechanics, each particle is still represented by a material point  $\underline{\mathbf{X}}$ , but its kinematic*

properties are defined in a more refined way. At the microscopic level of observation, a particle appears itself as a continuum  $V(\underline{\mathbf{X}})$  of small extent. Let us call  $\underline{\mathbf{X}}$  its center of mass and  $\underline{\mathbf{x}}$  a point of  $V(\underline{\mathbf{X}})$ . As  $V(\underline{\mathbf{X}})$  is of small extent, it is natural to look at the Taylor expansion of the local displacement  $\underline{\mathbf{u}}(\underline{\mathbf{x}})$  with respect to  $\underline{\mathbf{x}} - \underline{\mathbf{X}}$  and also, as a first approximation, to stop this expansion with the terms of degree 1:

$$\underline{\mathbf{u}}(\underline{\mathbf{x}}, \underline{\mathbf{X}}) = \underline{\mathbf{U}}(\underline{\mathbf{X}}) + \underline{\chi} \cdot (\underline{\mathbf{x}} - \underline{\mathbf{X}}) \quad (18)$$

The physical significance of this assumption is clear: one postulates that one can get a sufficient description of the relative motion of the various points of the particle if one assumes that this relative motion is a homogeneous deformation. For a given local field  $\underline{\mathbf{u}}(\underline{\mathbf{x}}, \underline{\mathbf{X}})$ , in short  $\underline{\mathbf{u}}(\underline{\mathbf{x}})$ , instead of explicitly performing the aforementioned Taylor expansion, it has been proposed in (Forest and Sab, 1998; Forest, 2002; Jänicke et al., 2009) to determine the homogeneous deformation field (18) that is the closest to the actual displacement field, in the sense of the following minimisation problem:

$$\min_{\underline{\mathbf{U}}(\underline{\mathbf{X}}), \underline{\chi}(\underline{\mathbf{X}})} \int_{V(\underline{\mathbf{X}})} \left\| \underline{\mathbf{u}}(\underline{\mathbf{x}}) - \underline{\mathbf{U}}(\underline{\mathbf{X}}) - \underline{\chi}(\underline{\mathbf{X}}) \cdot (\underline{\mathbf{x}} - \underline{\mathbf{X}}) \right\|^2 dV \quad (19)$$

for a given material point  $\underline{\mathbf{X}}$ . The minimisation procedure is straightforward and delivers, taking  $\underline{\mathbf{X}}$  as the centre of  $V(\underline{\mathbf{X}})$ :

$$\underline{\mathbf{U}}(\underline{\mathbf{X}}) = \langle \underline{\mathbf{u}}(\underline{\mathbf{x}}) \rangle_{V(\underline{\mathbf{X}})} \quad (20)$$

$$\begin{aligned} \underline{\chi}(\underline{\mathbf{X}}) &= \langle (\underline{\mathbf{u}}(\underline{\mathbf{x}}) - \underline{\mathbf{U}}(\underline{\mathbf{X}})) \otimes (\underline{\mathbf{x}} - \underline{\mathbf{X}}) \rangle_{V(\underline{\mathbf{X}})} \cdot \underline{\mathbf{A}}^{-1} \\ &= \langle \underline{\mathbf{u}}(\underline{\mathbf{x}}) \otimes (\underline{\mathbf{x}} - \underline{\mathbf{X}}) \rangle_{V(\underline{\mathbf{X}})} \cdot \underline{\mathbf{A}}^{-1} \end{aligned} \quad (21)$$

with

$$\underline{\mathbf{A}} = \langle (\underline{\mathbf{x}} - \underline{\mathbf{X}}) \otimes (\underline{\mathbf{x}} - \underline{\mathbf{X}}) \rangle_{V(\underline{\mathbf{X}})} \quad (22)$$

The relation (20) is known from classical homogenisation methods and defines the macroscopic displacement as the zeroth moment of the local displacement field. Formula (21) has the merit to unambiguously define the macroscopic micromorphic degrees of freedom as the first moment of the local displacement field, tensor  $\underline{\mathbf{A}}$  being the quadratic moment tensor of the unit cell. This represents an enhancement of the macroscopic description that incorporates additional effects of the microstructure compared to conventional schemes.

If the displacement field is a linear transformation,  $\underline{\mathbf{u}} = \underline{\mathbf{E}} \cdot \underline{\mathbf{x}}$ , the microdeformation is computed as

$$\chi_{ij} = \langle u_i x_k \rangle A_{kj}^{-1} = \langle E_{il} x_l x_k \rangle A_{kj}^{-1} = E_{il} \langle x_l x_k \rangle A_{kj}^{-1} = E_{ij} \quad (23)$$

so that the microdeformation coincides with the macro-deformation  $\underline{\mathbf{E}}$ . In particular, if a rigid body motion is applied to the unit cell, the microdeformation will reduce to the applied rotation, as it should be.

### 3.2 Higher order strain measures

The mechanical theory requires the evaluation of the macroscopic gradients of the degrees of freedom. The macroscopic gradient of the displacement field is still given by the averaging relation:

$$\underline{\mathbf{U}} \otimes \nabla_{\mathbf{X}} = \langle \underline{\mathbf{u}} \otimes \nabla_{\mathbf{x}} \rangle_{V(\underline{\mathbf{X}})} \quad (24)$$

The gradient of the microdeformation (15) is computed using the definition (21) as follows:

$$\begin{aligned} K_{ijk} &= \frac{\partial}{\partial X_k} \left( \langle (u_i - U_i)(x_l - X_l) \rangle A_{lj}^{-1} \right) \\ &= \langle \frac{\partial}{\partial x_k} ((u_i - U_i)(x_l - X_l)) \rangle A_{lj}^{-1} \\ &\quad + \langle (u_i - U_i)(x_l - X_l) \rangle \frac{\partial}{\partial X_k} A_{lj}^{-1} \\ &= \langle u_{i,k}(x_l - X_l) \rangle A_{lj}^{-1} + \langle (u_i - U_i) \rangle A_{kj}^{-1} \\ &\quad + \langle (u_i - U_i)(x_l - X_l) \rangle A_{lj,k}^{-1} \end{aligned} \quad (25)$$

Taking (20) into account, and assuming that  $\underline{\mathbf{A}}$  does not vary from material point to material point, the microdeformation gradient takes the simple form:

$$\underline{\mathbf{K}}^T(\underline{\mathbf{X}}) = \langle \underline{\mathbf{u}}(\underline{\mathbf{x}}) \otimes \nabla_{\mathbf{x}} \otimes (\underline{\mathbf{x}} - \underline{\mathbf{X}}) \rangle \cdot \underline{\mathbf{A}}^{-1}, \quad K_{ijk} = \langle u_{i,k}(x_l - X_l) \rangle A_{lj}^{-1} \quad (26)$$

where transposition of the third rank tensor is applied to the last two indices. Accordingly, the microdeformation gradient can be interpreted as the first moment of the distribution of the local displacement gradient.

The relative deformation must also be evaluated and takes the form of the difference:

$$\underline{\mathbf{e}}(\underline{\mathbf{X}}) = \langle \underline{\mathbf{u}}(\underline{\mathbf{x}}) \otimes \nabla_{\mathbf{x}} \rangle_{V(\underline{\mathbf{X}})} - \langle \underline{\mathbf{u}}(\underline{\mathbf{x}}) \otimes (\underline{\mathbf{x}} - \underline{\mathbf{X}}) \rangle_{V(\underline{\mathbf{X}})} \cdot \underline{\mathbf{A}}^{-1} \quad (27)$$

When the displacement field  $\underline{\mathbf{u}}$  is a linear transformation, including rigid body motions, both the relative deformation and the microdeformation gradient vanish, as it should be.

### 3.3 Polynomial Ansatz

Quadratic Ansätze have been initially proposed in (Gologanu et al., 1997; Forest, 1998; Kruch and Forest, 1998; Forest and Sab, 1998; Enakoutsa and Leblond, 2009) to extend the usual affine conditions of loading of the material volume element in order to incorporate strain gradient effects in the homogenisation procedure. Such polynomial developments represent an alternative to multiscale asymptotic expansions to derive effective higher order properties (Boutin, 1996), with the advantage that they can be used in a straightforward manner, irrespective of the local linear or nonlinear behaviour of the composite material.

We consider the following polynomial Ansatz of degree 4:

$$u_i^*(\underline{\mathbf{x}}) = E_{ij}x_j + \frac{1}{2}D_{ijk}x_jx_k + \frac{1}{3}D_{ijkl}x_jx_kx_l + \frac{1}{4}D_{ijklm}x_jx_kx_lx_m, \forall \underline{\mathbf{x}} \in V(0) \quad (28)$$

that is written in the following intrinsic form:

$$\begin{aligned} \underline{\mathbf{u}}^*(\underline{\mathbf{x}}) &= \underline{\mathbf{E}} \cdot \underline{\mathbf{x}} + \frac{1}{2} \underline{\underline{\mathbf{D}}} : (\underline{\mathbf{x}} \otimes \underline{\mathbf{x}}) + \frac{1}{3} \underline{\underline{\underline{\mathbf{D}}}} : (\underline{\mathbf{x}} \otimes \underline{\mathbf{x}} \otimes \underline{\mathbf{x}}) \\ &+ \frac{1}{4} \underline{\underline{\underline{\underline{\mathbf{D}}}}} :: (\underline{\mathbf{x}} \otimes \underline{\mathbf{x}} \otimes \underline{\mathbf{x}} \otimes \underline{\mathbf{x}}), \quad \forall \underline{\mathbf{x}} \in V(0) \end{aligned} \quad (29)$$

where the coefficients are tensors of ranks 2 to 5.

The macroscopic micromorphic strain measures are now computed successively for such a polynomial field on the reference unit cell  $V(0)$ :

$$\langle \underline{\mathbf{u}}^* \otimes \nabla_{\underline{\mathbf{x}}} \rangle_{V(0)} = \underline{\mathbf{E}} + \underline{\underline{\mathbf{D}}} : \underline{\underline{\mathbf{A}}} \quad (30)$$

$$\underline{\underline{\underline{\chi}}} = \langle \underline{\mathbf{u}}^* \otimes \underline{\mathbf{x}} \rangle_{V(0)} \cdot \underline{\underline{\mathbf{A}}}^{-1} = \underline{\mathbf{E}} + \frac{1}{3} \underline{\underline{\underline{\mathbf{D}}}} : \underline{\underline{\underline{\mathbf{A}}}} \cdot \underline{\underline{\underline{\mathbf{A}}}}^{-1}, \chi_{ij} = E_{ij} + \frac{1}{3} D_{ipqr} A_{pqrk} A_{kj}^{-1} \quad (31)$$

$$\underline{\underline{\underline{\underline{\mathbf{K}}}}}^T = \underline{\underline{\underline{\underline{\mathbf{D}}}}} + \underline{\underline{\underline{\underline{\mathbf{D}}}}} : \underline{\underline{\underline{\underline{\mathbf{A}}}}} \cdot \underline{\underline{\underline{\underline{\mathbf{A}}}}}^{-1}, K_{ipq} = \langle u_{i,q} x_r \rangle_{V(0)} A_{rp}^{-1} = D_{iqp} + D_{ijklm} A_{klmr} A_{rp}^{-1} \quad (32)$$

These simple formula hold if the coordinate system is such that  $\langle \underline{\mathbf{x}} \rangle = \underline{\underline{\mathbf{X}}} = \underline{\underline{\mathbf{0}}}$ , and that the means  $\langle x_i \rangle$ ,  $\langle x_i x_j x_k \rangle$  and  $\langle x_i x_j x_k x_l x_m \rangle$  identically vanish. The fourth order geometric moment  $\underline{\underline{\underline{\underline{\mathbf{A}}}}}$  of the unit cell has been introduced:

$$\underline{\underline{\underline{\underline{\mathbf{A}}}}} = \langle \underline{\mathbf{x}} \otimes \underline{\mathbf{x}} \otimes \underline{\mathbf{x}} \otimes \underline{\mathbf{x}} \rangle_{V(0)} \quad (33)$$

It is interesting to notice that the relative deformation is related only to the third order polynomial:

$$\underline{\epsilon} = \underline{D} : \underline{A} - \frac{1}{3} \underline{D} : \underline{A} \cdot \underline{A}^{-1} \quad (34)$$

The formula (30) to (32) set direct linear relationships between the coefficients of the polynomial and the strain measures of the effective micromorphic medium. They were used in Jänicke et al. (2009) to prescribe a given curvature  $\underline{K}$  or relative deformation to the unit cell. However the number of coefficients in the polynomials generally differs from the number of components of the generalised strain measures. For instance, the microdeformation gradient  $K_{ipq}$  cannot be controlled solely by the coefficients  $D_{ipq}$  of the quadratic polynomial since  $D_{ipq}$  is symmetric with respect to the last two indices contrary to  $K_{ipq}$ . The selection of the relevant higher order polynomial coefficients remains to be done. In the present contribution, we will only consider the coefficients  $D_{ijk}$  and some coefficients of  $D_{ijkl}$ .

However, the polynomial (29) will usually not be applied to the whole volume but instead at the boundary  $\partial V$  of a given heterogeneous material volume element  $V$ :

$$\begin{aligned} \underline{u}(\underline{x}) &= \underline{E} \cdot \underline{x} + \frac{1}{2} \underline{D} : (\underline{x} \otimes \underline{x}) + \frac{1}{3} \underline{D} : (\underline{x} \otimes \underline{x} \otimes \underline{x}) \\ &+ \frac{1}{4} \underline{D} :: (\underline{x} \otimes \underline{x} \otimes \underline{x} \otimes \underline{x}), \quad \forall \underline{x} \in \partial V \end{aligned} \quad (35)$$

In that case, the relation (30) is still valid but (32) must be modified. Note that the microdeformation cannot be controlled from the displacement prescribed at the boundary. The overall microdeformation gradient can be computed knowing the displacements prescribed at the boundary, using the same special coordinate system as previously, and choosing a constant translation such that  $\underline{U}(0) = 0$ :

$$\begin{aligned} K_{ipq} &= \frac{1}{V} A_{rp}^{-1} \int_{V(0)} u_{i,q} x_r dV = \frac{1}{V} A_{rp}^{-1} \int_{V(0)} (u_i x_r)_{,q} dV \\ &- \frac{1}{V} A_{qp}^{-1} \int_{V(0)} u_i dV \\ &= \frac{1}{V} A_{rp}^{-1} \int_{V(0)} (u_i x_r)_{,q} dV = \frac{1}{V} A_{rp}^{-1} \int_{\partial V(0)} u_i x_r n_q dS \\ &= \frac{1}{V} A_{rp}^{-1} \int_{\partial V(0)} u_i^* x_r n_q dS \\ &= \frac{1}{V} A_{rp}^{-1} \int_{V(0)} u_{i,q}^* x_r dV + \frac{1}{V} A_{qp}^{-1} \int_{V(0)} u_i^* dV \end{aligned} \quad (36)$$

so that the expression differs from (32) by the mean value of  $\underline{\mathbf{u}}^*$ . We find :

$$\underline{\underline{\mathbf{K}}}^T = \underline{\underline{\mathbf{D}}} + \underline{\underline{\mathbf{D}}} : \underline{\underline{\mathbf{A}}} \cdot \underline{\underline{\mathbf{A}}}^{-1} + \underline{\underline{\mathbf{D}}} : \underline{\underline{\mathbf{A}}} \otimes \underline{\underline{\mathbf{A}}}^{-1} + \underline{\underline{\mathbf{D}}} :: \underline{\underline{\mathbf{A}}} \otimes \underline{\underline{\mathbf{A}}}^{-1} \quad (37)$$

$$K_{ipq} = D_{iqp} + D_{iqklm} A_{klmr} A_{rp}^{-1} + D_{ijk} A_{jk} A_{qp}^{-1} + D_{ijklm} A_{jklm} A_{qp}^{-1} \quad (38)$$

Finally, the real local field will be the superposition of the polynomial and of a perturbation

$$\underline{\mathbf{u}}(\underline{\mathbf{x}}) = \underline{\mathbf{u}}^*(\underline{\mathbf{x}}) + \underline{\mathbf{v}}(\underline{\mathbf{x}}), \quad \forall \underline{\mathbf{x}} \in V \quad (39)$$

The fluctuation leads to additional contributions to the micromorphic measures that are obtained by substituting  $\underline{\mathbf{v}}$  to  $\underline{\mathbf{u}}$  in the formula (21), (26) and (27). These contributions do not vanish in general.

### 3.4 Identification of generalised effective elastic moduli

The identification procedure of the higher order elastic moduli is now presented based on an explicit example of a periodic composite material.

#### Definition of the chosen composite material

The chosen periodic composite material for the evaluation of the extended homogenisation methods is made of a hard isotropic linear elastic phase ( $h$ ) and a soft isotropic linear elastic phase ( $s$ ) :

$$E^h = 100000 \text{ MPa}, \quad \nu^h = 0.3, \quad E^s = 500 \text{ MPa}, \quad \nu^s = 0.3$$

The two phases display a contrast of 200 in their Young's modulus. The retained two-dimensional geometry of the unit cell  $V_0$  of the periodic composite is shown in figure 4. It exhibits orthotropic symmetry. The volume fraction of the hard phase is  $f^h = 0.424$ . The whole microstructure is obtained by plane tessellation in the defined directions 1 and 2.

#### Identification of classical elastic moduli

Classical periodic homogenisation is used to compute the orthotropic elastic properties of the effective Cauchy material. A constant mean deformation gradient  $E_{ij}$  is applied to the unit cell in which the displacement field is of the form :

$$\underline{\mathbf{u}}(\underline{\mathbf{x}}) = \underline{\underline{\mathbf{E}}} \cdot \underline{\mathbf{x}} + \underline{\mathbf{v}}(\underline{\mathbf{x}}) \quad (40)$$

where  $\underline{\mathbf{v}}$  is the periodic displacement fluctuation taking identical values at homologous points of the boundary  $\partial V_0$  of the unit cell. The effective moduli are determined from the mean elastic energy density induced by

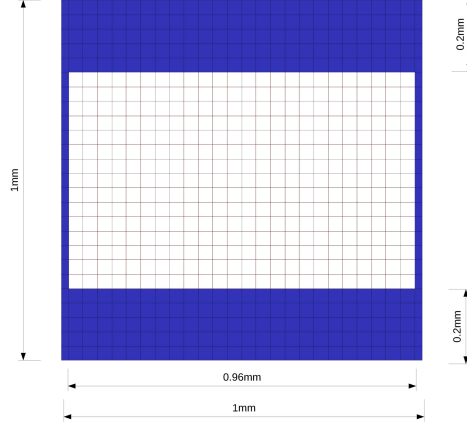


**Figure 4.** Unit cell  $V_0$  of the periodic composite material. The hard phase is red and the soft phase is blue. The orthotropy axes 1 and 2 are respectively horizontal and vertical.

three successive independent loading conditions, as illustrated in figure 5. Finite element simulations are performed under plane strain conditions. The found moduli are provided in table 2. They are defined in the following matrix form:

$$\begin{bmatrix} \Sigma_{11} \\ \Sigma_{22} \\ \Sigma_{12} \end{bmatrix} = \begin{bmatrix} C_{11} & C_{12} & 0 \\ C_{12} & C_{22} & 0 \\ 0 & 0 & C_{44} \end{bmatrix} \begin{bmatrix} E_{11} \\ E_{22} \\ 2E_{12} \end{bmatrix} \quad (41)$$

As a comparison, we have also computed the apparent effective moduli when homogeneous deformation boundary conditions are applied to the unit cell, i.e. when the fluctuation is taken to vanish :  $\underline{\mathbf{u}} = 0, \forall \underline{\mathbf{x}} \in \partial V_0$ . These boundary conditions are referred to as KUBC, kinematic uniform boundary

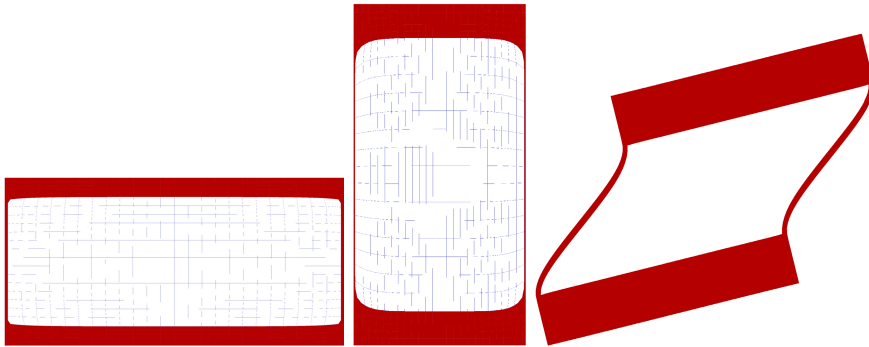


**Figure 5.** Loading conditions applied to the unit cell for the determination of the effective properties of the homogeneous equivalent Cauchy material. The first, second and third rows correspond to:  $E_{11} = 1, E_{22} = 1, E_{12} = E_{21} = 0.25$ , respectively. In each case the remaining components of  $E_{ij}$  vanish.

	$C_{11}$ (MPa)	$C_{12}$ (MPa)	$C_{22}$ (MPa)	$C_{44}$ (MPa)
periodic	44748	1579	7163	372
KUBC	45707	3181	9920	6186

**Table 2.** Elastic properties of the effective Cauchy material.

conditions. The corresponding apparent moduli, also given in table 2, are significantly stiffer than effective moduli from periodic homogenisation, as expected (Kanit et al., 2003).

### RVE size for strain gradient overall properties

The influence of the fluctuation type introduced in the boundary conditions in the computations of the previous section clearly shows that there is undoubtedly a boundary layer effect due to the polynomial boundary conditions, see also (Forest and Trinh, 2011). To get rid of the boundary layer effect, it is proposed to consider volume elements containing an increasing number of unit cells, typically a collection of  $N \times N$  unit cells, with  $N = 1, 3, 5, \dots$  up to  $N = 27$  in the following simulations. We look for the size  $N$  for which the energy distribution in the bulk of the sample, defined as a zone of fixed size  $M \times M$ , does not vary any more when the polynomial

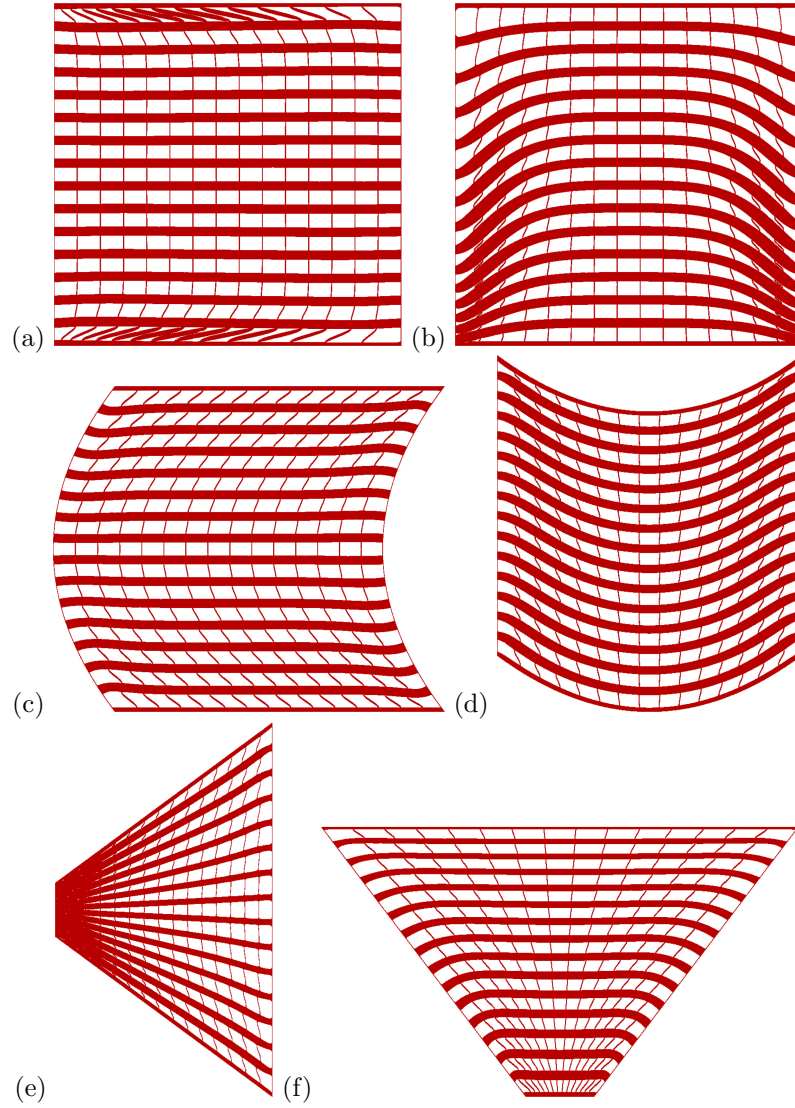


**Figure 6.** Deformation of a  $15 \times 15$ -cell volume elements corresponding to the following Dirichlet conditions at the outer boundary: (a)  $D_{111} : \underline{\mathbf{u}} = 1/2x_1^2\mathbf{e}_1$ , (b)  $D_{222} : \underline{\mathbf{u}} = 1/2x_2^2\mathbf{e}_2$ , (c)  $D_{122} : \underline{\mathbf{u}} = 1/2x_2^2\mathbf{e}_1$ , (d)  $D_{211} : \underline{\mathbf{u}} = 1/2x_1^2\mathbf{e}_2$ , (e)  $D_{212} : \underline{\mathbf{u}} = x_1x_2\mathbf{e}_2$ , (f)  $D_{112} : \underline{\mathbf{u}} = x_1x_2\mathbf{e}_1$ .

boundary conditions are applied at the remote boundary with the same given values of the polynomial coefficients. The obtained size will be called the RVE size for the considered polynomial conditions. In particular, the attention is focused on the energy density distribution inside the central unit cell ( $M = 1$ ).

In the case of affine boundary conditions used for classical homogenisation, such a procedure is known to lead to a stabilized periodic stress–strain field in the bulk of the volume element. In particular, the fluctuation at the boundary of a unit cell, defined as the difference between the displacement field and the affine contribution, is then found to be periodic. This is no longer the case for quadratic conditions (Forest and Trinh, 2011).

For more general polynomial Dirichlet conditions prescribed at the outer surface, we can investigate the convergence of the mechanical fields for an increasing window size. We also define, in a similar way, the fluctuation  $\underline{v}$  and examine its properties at the boundary of the central unit cell. This program has been performed in the reference (Forest and Trinh, 2011) for a cubic grid–like composite material for quadratic polynomials. We apply it to the orthotropic microstructure of figure 4 considered in this work. We use it also to determine the corresponding overall second gradient properties and compare them with the estimations based on an *a priori* choice of the fluctuation. The analysis is limited to the quadratic polynomial term. That is why only strain gradient properties will be identified and not the full micromorphic ones.

The six 2D deformation modes corresponding to a full quadratic polynomial in equation (35):  $D_{111}, D_{222}, D_{122}, D_{211}, D_{212}, D_{112}$  are considered. The associated deformed 15x15–cell volume elements are shown in figure 6. The converged shapes of the central unit cell extracted from the previous volume elements are given in figure 6, for the same magnification. The modes  $D_{111}, D_{222}$  and  $D_{122}$  induce only limited deformation in the central unit cell whereas  $D_{211}, D_{212}, D_{112}$  involve significant straining. The elastic energy density levels  $\langle \underline{\sigma} : \underline{\varepsilon} \rangle_{V_0}$  over the central unit cell  $V_0$  associated with these six modes are given in table 3 depending on the size  $N$  of the volume element. Convergence to finite energy values is obtained for the modes  $D_{211}, D_{212}, D_{112}$  whereas the material turns out to be insensitive to the modes  $D_{111}, D_{222}$  and  $D_{122}$ .

The displayed convergence for the considered collection of cells ensures that a representative size has been reached. However, quite a large number of cells is necessary to detect the energy–free modes. Detailed analysis confirms that the fluctuation corresponding to the central unit cell response is not periodic, as pointed out by Forest and Trinh (2011).

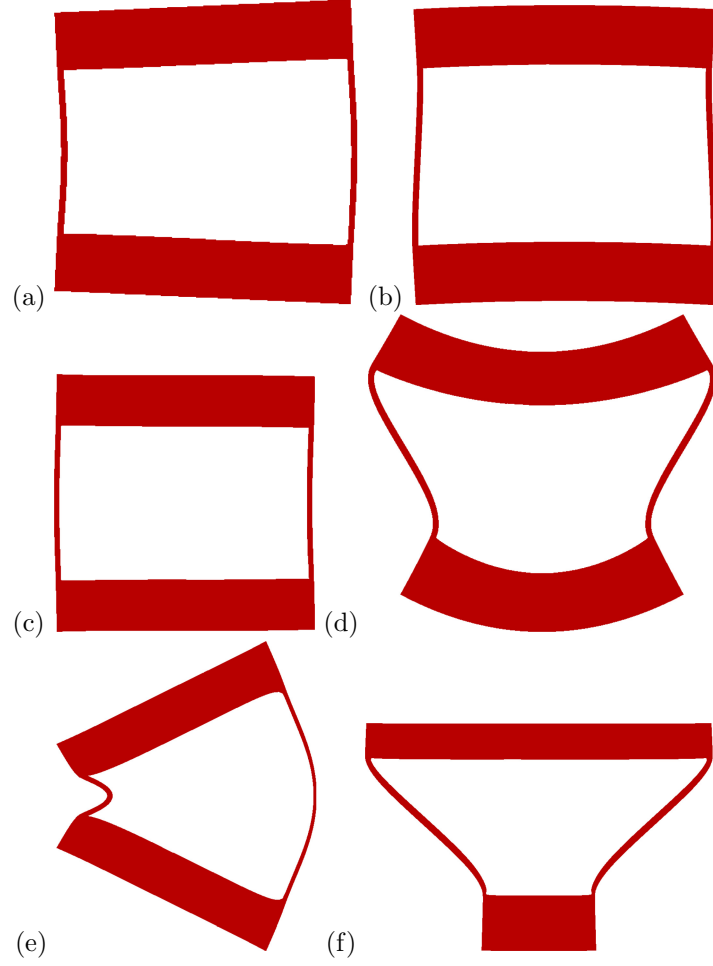


**Figure 7.** Shape of the central cell of a 15x15 volume element subjected to the following Dirichlet boundary conditions: (a)  $D_{111} : \underline{\mathbf{u}} = 1/2x_1^2 \underline{\mathbf{e}}_1$ , (b)  $D_{222} : \underline{\mathbf{u}} = 1/2x_2^2 \underline{\mathbf{e}}_2$ , (c)  $D_{122} : \underline{\mathbf{u}} = 1/2x_2^2 \underline{\mathbf{e}}_1$ , (d)  $D_{211} : \underline{\mathbf{u}} = 1/2x_1^2 \underline{\mathbf{e}}_2$ , (e)  $D_{212} : \underline{\mathbf{u}} = x_1x_2 \underline{\mathbf{e}}_2$ , (f)  $D_{112} : \underline{\mathbf{u}} = x_1x_2 \underline{\mathbf{e}}_1$ .

NxN-cell	$D_{111} = 1$	$D_{122} = 1$	$D_{212} = 1$	$D_{112} = 1$	$D_{211} = 1$	$D_{222} = 1$
3x3	3	19	1033	527	368	324
7x7	2	0.12	789	6176	660	227
9x9	1.3	0.3	761	6079	565	89
11x11	0.9	0.4	759	5930	474	27
15x15	0.5	0.33	770	5714	371	1.8
21x21	0.4	0.32	776	5587	325	0.2
27x27	0.33	0.32	777	5548	315	0.2

**Table 3.** Average elastic energy density in the central unit of NxN-cell volume elements submitted to quadratic Dirichlet boundary conditions. The components  $D_{ijk}$  are given in  $\text{mm}^{-1}$  and the elastic energy values are in MPa.

### Identification of second gradient effective elastic moduli

The quadratic polynomial loading conditions  $D_{ijk}$  can be used to identify the elastic properties of an overall second gradient medium. The simple force stress tensor  $\underline{\Sigma}$  is still related to the strain tensor  $\underline{\mathcal{E}}$  by the moduli (41). In a medium exhibiting point symmetry, the double stress tensor  $M_{ijk} = M_{ikj}$  is linearly related to the second gradient of displacement  $K_{ijk} = K_{ikj}$  by the matrix of double elasticity moduli. The structure of anisotropic six rank tensors of strain gradient elasticity was analysed by Auffray et al. (2009, 2010). In the most general situation the associated matricial representation is written:

$$\mathbf{M} = [\mathbf{A}]\mathbf{K} \quad (42)$$

with

$$\mathbf{M} = \begin{bmatrix} M_{111} \\ M_{122} \\ \sqrt{2}M_{212} \\ M_{222} \\ M_{211} \\ \sqrt{2}M_{121} \end{bmatrix}, \quad \mathbf{K} = \begin{bmatrix} K_{111} \\ K_{122} \\ K_{212} \\ K_{222} \\ K_{211} \\ K_{121} \end{bmatrix}$$

$$[\mathbf{A}] = \begin{bmatrix} A_{111111} & A_{111122} & \sqrt{2}A_{111212} & A_{111222} & A_{111211} & \sqrt{2}A_{111121} \\ A_{122111} & A_{122122} & \sqrt{2}A_{122212} & A_{122222} & A_{122211} & \sqrt{2}A_{122121} \\ \sqrt{2}A_{212111} & \sqrt{2}A_{212122} & 2A_{212122} & \sqrt{2}A_{212222} & \sqrt{2}A_{212211} & 2A_{212121} \\ A_{222111} & A_{222122} & \sqrt{2}A_{222212} & A_{222222} & A_{222211} & \sqrt{2}A_{222121} \\ A_{211111} & A_{211122} & \sqrt{2}A_{211212} & A_{211222} & A_{211211} & \sqrt{2}A_{211121} \\ \sqrt{2}A_{121111} & \sqrt{2}A_{121122} & 2A_{121212} & \sqrt{2}A_{121222} & \sqrt{2}A_{121211} & 2A_{121121} \end{bmatrix}$$

This notation, using square root of two before  $K_{212}$  and  $M_{212}$ , defines a true second order tensorial representation of the sixth-order tensor of double elasticity. Ranking the components of the second gradient of displacement

as proposed in the former matricial representation, leads, in the orthotropic case, to the uncoupled system:

$$\begin{bmatrix} M_1 \\ M_2 \\ M_3 \\ M_4 \\ M_5 \\ M_6 \end{bmatrix} = \begin{bmatrix} A_{11} & A_{12} & A_{13} & 0 & 0 & 0 \\ A_{12} & A_{22} & A_{23} & 0 & 0 & 0 \\ A_{13} & A_{23} & A_{33} & 0 & 0 & 0 \\ 0 & 0 & 0 & A_{44} & A_{45} & A_{46} \\ 0 & 0 & 0 & A_{45} & A_{55} & A_{56} \\ 0 & 0 & 0 & A_{46} & A_{56} & A_{66} \end{bmatrix} \begin{bmatrix} K_1 \\ K_2 \\ K_3 \\ K_4 \\ K_5 \\ K_6 \end{bmatrix} \quad (43)$$

with the simplified notations :

$$[K_1 \ K_2 \ K_3 \ K_4 \ K_5 \ K_6] = [K_{111} \ K_{122} \ \sqrt{2}K_{212} \ K_{222} \ K_{211} \ \sqrt{2}K_{121}],$$

$$[M_1 \ M_2 \ M_3 \ M_4 \ M_5 \ M_6] = [M_{111} \ M_{122} \ \sqrt{2}M_{212} \ M_{222} \ M_{211} \ \sqrt{2}M_{121}]$$

and

$$[A_{11} \ A_{12} \ A_{13} \ A_{22} \ A_{23} \ A_{33}] =$$

$$[A_{111111} \ A_{111122} \ \sqrt{2}A_{111212} \ A_{122122} \ \sqrt{2}A_{122212} \ 2A_{212212}],$$

$$[A_{44} \ A_{45} \ A_{46} \ A_{55} \ A_{56} \ A_{66}] =$$

$$[A_{222222} \ A_{222211} \ \sqrt{2}A_{222121} \ A_{211211} \ \sqrt{2}K_{211121} \ 2K_{121121}]$$

This makes 12 independent double elasticity moduli to be identified from the analysis of the response of the unit cell to non-homogeneous loading conditions. Twelve loading conditions are needed to identify them corresponding to twelve sets of the values of the coefficients  $D_{ijk}$ . The six selected loading conditions are labeled ( $a, b, c, d, e, f$ ) for the identification of the first block of 6 constants in the matrix (43), taking advantage of the orthotropic symmetry of the material. Six additional ones are needed for the second block. For each loading, the post-processing procedure yields the mean energy density  $2\epsilon = \langle \boldsymbol{\sigma} : \boldsymbol{\varepsilon} \rangle_{V_0}$  in the unit cell and the overall curvature  $K_1, K_2$  and  $K_3$ . The mean energy density is related to the overall energy density in the form:

$$2\epsilon = \begin{bmatrix} K_1 \\ K_2 \\ K_3 \\ K_4 \\ K_5 \\ K_6 \end{bmatrix}^T \begin{bmatrix} A_{11} & A_{12} & A_{13} & 0 & 0 & 0 \\ A_{12} & A_{22} & A_{23} & 0 & 0 & 0 \\ A_{13} & A_{23} & A_{33} & 0 & 0 & 0 \\ 0 & 0 & 0 & A_{44} & A_{45} & A_{46} \\ 0 & 0 & 0 & A_{45} & A_{55} & A_{56} \\ 0 & 0 & 0 & A_{46} & A_{56} & A_{66} \end{bmatrix} \begin{bmatrix} K_1 \\ K_2 \\ K_3 \\ K_4 \\ K_5 \\ K_6 \end{bmatrix} \quad (44)$$

$A_{11}$ (MPa.mm <sup>2</sup> )	$A_{22}$ (MPa.mm <sup>2</sup> )	$A_{33}$ (MPa.mm <sup>2</sup> )	$A_{12}$ MPa.mm <sup>2</sup>	$A_{23}$ MPa.mm <sup>2</sup>	$A_{13}$ MPa.mm <sup>2</sup>
134601	37436	124 548	68706	67368	127 213
$A_{44}$	$A_{55}$	$A_{66}$	$A_{45}$	$A_{46}$	$A_{56}$
69445	2801	32 175	40762	11 094	7 548

**Table 4.** Higher order elastic properties of the overall second-gradient material for the unit cell of figure 4(a). The fluctuation is taken to vanish at the unit cell boundary.

The found higher order moduli are listed in table 4 for a vanishing fluctuation  $\underline{v}$  in (35) at the boundary of the unit cell  $V_0$ . We have not determined the effective moduli corresponding to the converged states of the unit cell embedded in a  $N \times N$ -cell volume element in the sense of section 3.4, because zero-energy modes were detected as discussed above, so that the previous system of equations is undetermined. A specific procedure is necessary to determine the vanishing terms of the overall matrix.

### 3.5 Validation of the extended homogenisation method

The performance of the generalised overall properties determined in the previous section is evaluated by considering a reference problem for a structure made of a small number of unit cells of the type of 4(a). The limitation of the Cauchy continuum is first illustrated and improvements by means of a strain gradient substitution medium are presented.

We consider the composite structure made of  $10 \times 5$  cells of figure 8 (left). The following boundary value problem is considered on this structure. The left side of the structure is clamped, meaning that  $U_1 = U_2 = 0$ . The horizontal lower and upper sides are free of forces. The vertical displacement component  $U_2 = 1$  mm is prescribed on the right side, the component  $U_1$  being left free. The corresponding deformed shape of the structure is shown in figure 8 (right). It displays a combination of pure shear and bending modes in a boundary layer on the left side.

The same boundary value problem is considered for a homogeneous substitution Cauchy medium endowed with the elastic properties of table 2. The same clamping boundary conditions  $U_1 = U_2 = 0$  are prescribed on the left side. The bottom picture of Fig. 8 shows that the Cauchy medium does not capture the bending mode of the composite structure and only provides the shearing mode. This fact had already been noticed for laminates in (Forest and Sab, 1998; Forest and Trinh, 2011).

When the structure is made of a homogeneous second gradient medium

endowed with the properties of table 4, the deformed state and quantitative comparison in figure 9 show that the strain gradient effective medium fully captures the actual shear and bending modes. In figure 9, the displacement profile  $U_2(x_1)$  is given along the horizontal line close to the mid-section of the structure, as drawn in figure 8.

The simulation for second gradient elasticity is made by means of a micromorphic formulation for which penalty terms ensure that the microdeformation coincides with the gradient of the displacement field. Clamping was imposed through the prescription of vanishing microdeformation on the left side. Note that the choice of the additional boundary conditions on the left side is quite heuristic, as it is the case in most beam and plate models.

Note that an effective Cosserat continuum, for which the effective moduli can be determined in the same way, performs as good as the strain gradient model as shown in Fig. 9. More elaborate examples of loading must be developed in the future to select the best-suited generalised homogeneous equivalent continuum.

## 4 Homogenization of micromorphic media

The homogenisation schemes in this section must be clearly distinguished from the one of previous section since we consider here a generalised continuum model at both the microscopic and macroscopic levels. For instance, homogenisation of Cosserat composites were considered in (Forest et al., 2001; Liu and Hu, 2003; Xun et al., 2004).

The motivation for the development of homogenisation methods for mixtures of micromorphic media is mainly related to crystal plasticity. The mechanical behaviour of metallic polycrystals is notably size dependent and the conventional crystal plasticity framework fails at convincingly predict grain and precipitate size effects (Aslan et al., 2011). Single crystals can be regarded as Cosserat, strain gradient or micromorphic continua. It follows that a polycrystal is a heterogeneous generalised continuum for which specific homogenisation methods must be designed.

### 4.1 Multiscale asymptotic expansion method

In contrast to the previous part, the heterogeneous medium is now a mixture of micromorphic constituents, i.e. a heterogeneous micromorphic medium. One investigates the nature of the resulting homogeneous equivalent medium by means of asymptotic methods. The multiscale asymptotic method by Sanchez-Palencia (1974) is especially adequate for this purpose since, in contrast to the work done in the previous part, the nature of the

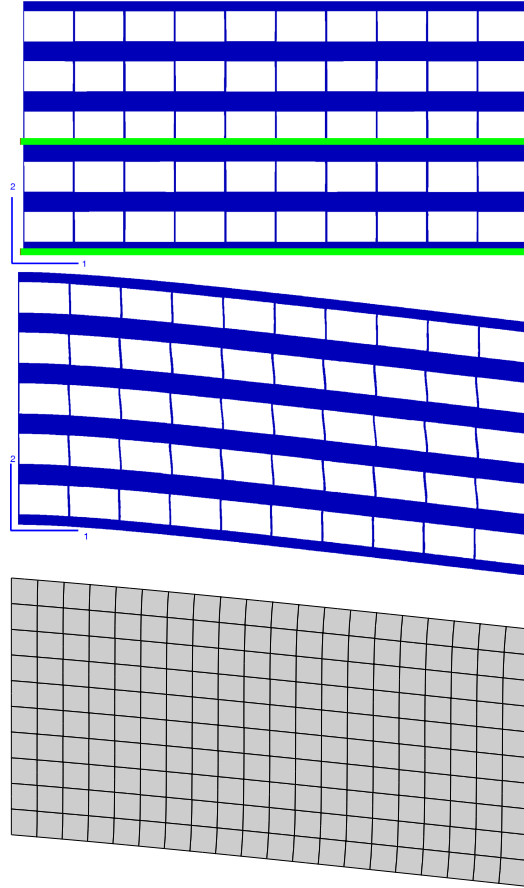


**Figure 8.** Reference composite structure made of 10x5 cells (left) and reference deformed shape of the structure. Two horizontal lines are shown on the structure for post-processing purposes. The bottom figure shows the deformed state predicted by the homogeneous equivalent Cauchy continuum.

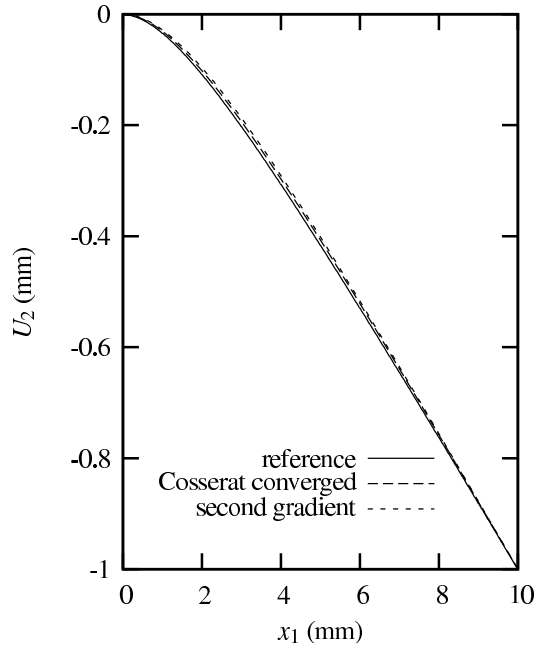


**Figure 9.** Vertical displacement component  $U_2$  along the mid-line visible in figure 8 as computed for the reference structure and Cosserat and strain gradient substitution media.

effective medium is not postulated *a priori* but rather is the result of the analysis.

The balance and constitutive equations of the micromorphic continuum are recalled briefly in the linear elastic framework for which the asymptotic methods can be applied in a straightforward manner (Forest et al., 2001) The motion of a micromorphic body  $\Omega$  is described by two independent sets of degrees of freedom : the displacement  $\underline{\mathbf{u}}$  and the micro-deformation  $\underline{\underline{\chi}}$  attributed to each material point. The micro-deformation accounts for the rotation and distortion of a triad associated with the underlying microstructure Eringen (1999). The micro-deformation can be split into its symmetric and skew-symmetric parts :

$$\underline{\underline{\chi}} = \underline{\underline{\chi}}^s + \underline{\underline{\chi}}^a \quad (45)$$

that are called respectively the micro-strain and the Cosserat rotation. The

associated deformation fields are the classical strain tensor  $\underline{\underline{\varepsilon}}$ , the relative deformation  $\underline{\underline{e}}$  and the micro-deformation gradient tensor  $\underline{\underline{\kappa}}$  defined by :

$$\underline{\underline{\varepsilon}} = \underline{\underline{\mathbf{u}}} \otimes^s \underline{\underline{\nabla}}, \quad \underline{\underline{e}} = \underline{\underline{\mathbf{u}}} \otimes \underline{\underline{\nabla}} - \underline{\underline{\chi}}, \quad \underline{\underline{\kappa}} = \underline{\underline{\chi}} \otimes \underline{\underline{\nabla}} \quad (46)$$

The symmetric part of  $\underline{\underline{e}}$  corresponds to the difference of material strain and micro-strain, whereas its skew-symmetric part accounts for the relative rotation of the material with respect to microstructure. The micro-deformation gradient can be split into two contributions :

$$\underline{\underline{\kappa}} = \underline{\underline{\kappa}}^s + \underline{\underline{\kappa}}^a, \quad \text{with} \quad \underline{\underline{\kappa}}^s = \underline{\underline{\chi}}^s \otimes \underline{\underline{\nabla}}, \quad \underline{\underline{\kappa}}^a = \underline{\underline{\chi}}^a \otimes \underline{\underline{\nabla}} \quad (47)$$

In this section, the analysis is restricted to small deformations, small micro-rotations, small micro-strains and small micro-deformation gradients. The statics of the micromorphic continuum is described by the symmetric force-stress tensor  $\underline{\underline{\sigma}}$ , the generally non-symmetric relative force-stress tensor  $\underline{\underline{s}}$  and third-rank stress tensor  $\underline{\underline{m}}$ . These tensors must fulfill the local form of the balance equations in the static case, in the absence of body simple nor double forces for simplicity :

$$(\underline{\underline{\sigma}} + \underline{\underline{s}}) \cdot \underline{\underline{\nabla}} = 0, \quad \underline{\underline{m}} \cdot \underline{\underline{\nabla}} + \underline{\underline{s}} = 0 \text{ on } \Omega \quad (48)$$

The constitutive equations for linear elastic centro-symmetric micromorphic materials read :

$$\underline{\underline{\sigma}} = \underline{\underline{a}} : \underline{\underline{\varepsilon}}, \quad \underline{\underline{s}} = \underline{\underline{b}} : \underline{\underline{e}}, \quad \underline{\underline{m}} = \underline{\underline{c}} : \underline{\underline{\kappa}} \quad (49)$$

The elasticity tensors display the major symmetries :

$$a_{ijkl} = a_{klij}, \quad b_{ijkl} = b_{klij}, \quad c_{ijkpqr} = c_{pqrijk} \quad (50)$$

and  $\underline{\underline{a}}$  has also the usual minor symmetries. The last constitutive law can be written in the form :

$$\underline{\underline{m}} = \underline{\underline{c}}^s : \underline{\underline{\kappa}}^s + \underline{\underline{c}}^a : \underline{\underline{\kappa}}^a \quad (51)$$

For the sake of simplicity, the tensors  $\underline{\underline{c}}^s$  and  $\underline{\underline{c}}^a$  are supposed to fulfill the conditions :

$$c_{ijkpqr}^s = c_{jikpqr}^s, \quad c_{ijkpqr}^a = -c_{jikpqr}^a \quad (52)$$

thus assuming that there is no coupling between the contributions of the symmetric and skew-symmetric parts of  $\underline{\underline{\chi}}$  to the third-rank stress tensor.

The setting of the boundary value problem on body  $\Omega$  is then closed by the boundary conditions. In the following, Dirichlet boundary conditions are considered of the form :

$$\underline{\mathbf{u}}(\underline{\mathbf{x}}) = 0, \quad \underline{\chi}(\underline{\mathbf{x}}) = 0, \quad \forall \underline{\mathbf{x}} \in \partial\Omega \quad (53)$$

where  $\partial\Omega$  denote the boundary of  $\Omega$ . The equations (46), (48), (49) and (53) define the boundary value problem  $\mathcal{P}$ .

The next sections of this work are restricted to micromorphic materials with periodic microstructure. The heterogeneous material is then obtained by space tessellation with cells translated from a single cell  $Y^l$ . The period of the microstructure is described by three dimensionless independent vectors  $(\underline{\mathbf{a}}_1, \underline{\mathbf{a}}_2, \underline{\mathbf{a}}_3)$  such that :

$$Y^l = \left\{ \underline{\mathbf{x}} = x_i \underline{\mathbf{a}}_i, |x_i| < \frac{l}{2} \right\}$$

where  $l$  is the characteristic size of the cell. We call  $\underline{\mathbf{a}}^l$ ,  $\underline{\mathbf{b}}^l$  and  $\underline{\mathbf{c}}^l$  the elasticity tensor fields of the periodic Cosserat material. They are such that :

$$\begin{aligned} \forall \underline{\mathbf{x}} \in \Omega, \forall (n_1, n_2, n_3) \in Z^3 / \underline{\mathbf{x}} + l(n_1 \underline{\mathbf{a}}_1 + n_2 \underline{\mathbf{a}}_2 + n_3 \underline{\mathbf{a}}_3) \in \Omega, \\ \underline{\mathbf{a}}^l(\underline{\mathbf{x}}) = \underline{\mathbf{a}}^l(\underline{\mathbf{x}} + l(n_1 \underline{\mathbf{a}}_1 + n_2 \underline{\mathbf{a}}_2 + n_3 \underline{\mathbf{a}}_3)), \\ \underline{\mathbf{b}}^l(\underline{\mathbf{x}}) = \underline{\mathbf{b}}^l(\underline{\mathbf{x}} + l(n_1 \underline{\mathbf{a}}_1 + n_2 \underline{\mathbf{a}}_2 + n_3 \underline{\mathbf{a}}_3)), \\ \underline{\mathbf{c}}^l(\underline{\mathbf{x}}) = \underline{\mathbf{c}}^l(\underline{\mathbf{x}} + l(n_1 \underline{\mathbf{a}}_1 + n_2 \underline{\mathbf{a}}_2 + n_3 \underline{\mathbf{a}}_3)) \end{aligned}$$

### Dimensional analysis

The size  $L$  of body  $\Omega$  is defined for instance as the maximum distance between two points. Dimensionless coordinates and displacements are introduced :

$$\underline{\mathbf{x}}^* = \frac{\underline{\mathbf{x}}}{L}, \quad \underline{\mathbf{u}}^*(\underline{\mathbf{x}}^*) = \frac{\underline{\mathbf{u}}(\underline{\mathbf{x}})}{L}, \quad \underline{\chi}^*(\underline{\mathbf{x}}^*) = \underline{\chi}(\underline{\mathbf{x}}) \quad (54)$$

The corresponding strain measures are :

$$\underline{\varepsilon}^*(\underline{\mathbf{x}}^*) = \underline{\mathbf{u}}^* \overset{s}{\otimes} \nabla^* \underline{\varepsilon}(\underline{\mathbf{x}}), \quad \underline{\mathbf{e}}^*(\underline{\mathbf{x}}^*) = \underline{\mathbf{u}}^* \otimes \nabla^* - \underline{\chi}^* = \underline{\mathbf{e}}(\underline{\mathbf{x}}) \quad (55)$$

$$\underline{\kappa}^*(\underline{\mathbf{x}}^*) = \underline{\chi}^* \otimes \nabla^* = L \underline{\kappa}(\underline{\mathbf{x}}) \quad (56)$$

and similarly

$$\underline{\underline{\boldsymbol{\kappa}}}^{s*}(\underline{\mathbf{x}}^*) = \underline{\underline{\boldsymbol{\chi}}}^{s*} \otimes \underline{\nabla}^* = L \underline{\underline{\boldsymbol{\kappa}}}^s(\underline{\mathbf{x}}), \quad \underline{\underline{\boldsymbol{\kappa}}}^{a*}(\underline{\mathbf{x}}^*) = \underline{\underline{\boldsymbol{\chi}}}^{a*} \otimes \underline{\nabla}^* = L \underline{\underline{\boldsymbol{\kappa}}}^a(\underline{\mathbf{x}}) \quad (57)$$

with  $\underline{\nabla}^* = \left( \frac{\partial \cdot}{\partial x_i^*} \right) \underline{\mathbf{e}}_i = L \underline{\nabla}$ . It is necessary to introduce next a norm of the elasticity tensors :

$$A = \underset{\underline{\mathbf{x}} \in Y^l}{\text{Max}} (|a_{ijkl}^l(\underline{\mathbf{x}})|, |b_{ijkl}^l(\underline{\mathbf{x}})|) \\ C^s = \underset{\underline{\mathbf{x}} \in Y^l}{\text{Max}} |c_{ijkpqr}^{sl}(\underline{\mathbf{x}})|, \quad C^a = \underset{\underline{\mathbf{x}} \in Y^l}{\text{Max}} |c_{ijkpqr}^{al}(\underline{\mathbf{x}})| \quad (58)$$

whereby characteristic lengths  $l_s$  and  $l_a$  can be defined as:

$$C^s = Al_s^2, \quad C^a = Al_a^2 \quad (59)$$

The definition of dimensionless stress and elasticity tensors follows :

$$\underline{\underline{\boldsymbol{\sigma}}}^*(\underline{\mathbf{x}}^*) = A^{-1} \underline{\underline{\boldsymbol{\sigma}}}(\underline{\mathbf{x}}), \quad \underline{\underline{\boldsymbol{\varepsilon}}}^*(\underline{\mathbf{x}}^*) = A^{-1} \underline{\underline{\boldsymbol{\varepsilon}}}(\underline{\mathbf{x}}), \quad \underline{\underline{\boldsymbol{m}}}^*(\underline{\mathbf{x}}^*) = (AL)^{-1} \underline{\underline{\boldsymbol{m}}}(\underline{\mathbf{x}}) \quad (60)$$

$$\underline{\underline{\boldsymbol{a}}}^*(\underline{\mathbf{x}}^*) = A^{-1} \underline{\underline{\boldsymbol{a}}}^l(\underline{\mathbf{x}}), \quad \underline{\underline{\boldsymbol{b}}}^*(\underline{\mathbf{x}}^*) = A^{-1} \underline{\underline{\boldsymbol{b}}}^l(\underline{\mathbf{x}}), \quad (61)$$

$$\underline{\underline{\boldsymbol{c}}}^{s*}(\underline{\mathbf{x}}^*) = (Al_c^2)^{-1} \underline{\underline{\boldsymbol{c}}}^{sl}(\underline{\mathbf{x}}), \quad \underline{\underline{\boldsymbol{c}}}^{a*}(\underline{\mathbf{x}}^*) = (Al_c^2)^{-1} \underline{\underline{\boldsymbol{c}}}^{al}(\underline{\mathbf{x}}) \quad (62)$$

Since the initial tensors  $\underline{\underline{\boldsymbol{a}}}^l, \underline{\underline{\boldsymbol{b}}}^l$  and  $\underline{\underline{\boldsymbol{c}}}^l$  are  $Y^l$ -periodic, the dimensionless counterparts are  $Y^*$ -periodic :

$$Y^* = \frac{l}{L} Y, \quad Y = \left\{ \underline{\mathbf{y}} = y_i \underline{\mathbf{e}}_i, |y_i| < \frac{1}{2} \right\} \quad (63)$$

$Y$  is the (dimensionless) unit cell used in the present asymptotic analyses. As a result, the dimensionless stress and strain tensors are related by the following constitutive equations :

$$\underline{\underline{\boldsymbol{\sigma}}}^* = \underline{\underline{\boldsymbol{a}}}^* : \underline{\underline{\boldsymbol{\varepsilon}}}^*, \quad \underline{\underline{\boldsymbol{s}}}^* = \underline{\underline{\boldsymbol{b}}}^* : \underline{\underline{\boldsymbol{\varepsilon}}}^*, \quad \underline{\underline{\boldsymbol{m}}}^* = \left( \frac{l_s}{L} \right)^2 \underline{\underline{\boldsymbol{c}}}^{s*} : \underline{\underline{\boldsymbol{\kappa}}}^{s*} + \left( \frac{l_a}{L} \right)^2 \underline{\underline{\boldsymbol{c}}}^{a*} : \underline{\underline{\boldsymbol{\kappa}}}^{a*} \quad (64)$$

The dimensionless balance equations read :

$$\forall \underline{\mathbf{x}}^* \in \Omega^*, \quad (\underline{\underline{\boldsymbol{\sigma}}}^* + \underline{\underline{\boldsymbol{s}}}^*) \cdot \underline{\nabla}^* = 0, \quad \underline{\underline{\boldsymbol{m}}}^* \cdot \underline{\nabla}^* + \underline{\underline{\boldsymbol{s}}}^* = 0 \quad (65)$$

A boundary value problem  $\mathcal{P}^*$  can be defined using equations (56), (64) and (65), complemented by the boundary conditions :

$$\forall \underline{\mathbf{x}}^* \in \partial\Omega^*, \quad \underline{\mathbf{u}}^*(\underline{\mathbf{x}}^*) = 0, \quad \underline{\underline{\boldsymbol{\chi}}}^*(\underline{\mathbf{x}}^*) = 0 \quad (66)$$

## The homogenisation problem

The boundary value problem  $\mathcal{P}^*$  is treated here as an element of a series of problems  $(\mathcal{P}_\epsilon)_{\epsilon>0}$  on  $\Omega^*$ . The homogenisation problem consists in the determination of the limit of this series when the dimensionless parameter  $\epsilon$ , regarded as small, tends towards 0. The series is chosen such that

$$\mathcal{P}_{\epsilon=\frac{1}{L}} = \mathcal{P}^*$$

The unknowns of boundary value problem  $\mathcal{P}_\epsilon$  are the displacement and micro-deformation fields  $\underline{\mathbf{u}}^\epsilon$  and  $\underline{\boldsymbol{\chi}}^\epsilon$  satisfying the following field equations on  $\Omega^*$  :

$$\underline{\boldsymbol{\sigma}}^\epsilon = \underline{\boldsymbol{\alpha}}^\epsilon : (\underline{\mathbf{u}}^\epsilon \otimes \nabla^*), \quad \underline{\boldsymbol{\xi}}^\epsilon = \underline{\boldsymbol{\beta}}^\epsilon : (\underline{\mathbf{u}}^\epsilon \otimes \nabla^* - \underline{\boldsymbol{\chi}}^\epsilon), \quad \underline{\boldsymbol{m}}^\epsilon = \underline{\boldsymbol{\zeta}}^\epsilon : (\underline{\boldsymbol{\chi}}^\epsilon \otimes \nabla^*) \quad (67)$$

$$(\underline{\boldsymbol{\sigma}}^\epsilon + \underline{\boldsymbol{\xi}}^\epsilon) \cdot \nabla^* = 0, \quad \underline{\boldsymbol{m}}^\epsilon \cdot \nabla^* + \underline{\boldsymbol{\xi}}^\epsilon = 0 \quad (68)$$

Different cases must now be distinguished depending on the relative position of the constitutive lengths  $l_s$  and  $l_a$  with respect to the characteristic lengths  $l$  and  $L$  of the problem. Four special cases are relevant for the present asymptotic analysis. The first case corresponds to a limiting process for which  $l_s/l$  and  $l_a/l$  remain constant when  $l/L$  goes to zero. The second case corresponds to the situation for which  $l_s/L$  and  $l_a/L$  remain constant when  $l/L$  goes to zero. The third (resp. fourth) situation assumes that  $l_s/l$  and  $l_a/L$  (resp.  $l_s/L$  and  $l_a/l$ ) remain constant when  $l/L$  goes to zero. These assumptions lead to four different homogenisation schemes labelled *HS1* to *HS4* in the sequel. The homogenisation scheme 1 (resp. 2) will be relevant when the ratio  $l/L$  is small enough and when  $l_s, l_a$  and  $l$  (resp.  $L$ ) have the same order of magnitude.

Accordingly, the following tensors of elastic moduli can be defined :

$$\underline{\boldsymbol{a}}^{(0)}(\underline{\mathbf{y}}) = \underline{\boldsymbol{a}}^* \left( \frac{l}{L} \underline{\mathbf{y}} \right), \quad \underline{\boldsymbol{b}}^{(0)}(\underline{\mathbf{y}}) = \underline{\boldsymbol{b}}^* \left( \frac{l}{L} \underline{\mathbf{y}} \right), \quad (69)$$

$$\underline{\boldsymbol{\zeta}}^{(1)}(\underline{\mathbf{y}}) = \left( \frac{l_s}{l} \right)^2 \underline{\boldsymbol{\zeta}}^* \left( \frac{l}{L} \underline{\mathbf{y}} \right), \quad \underline{\boldsymbol{\zeta}}^{(2)}(\underline{\mathbf{y}}) = \left( \frac{l_s}{L} \right)^2 \underline{\boldsymbol{\zeta}}^* \left( \frac{l}{L} \underline{\mathbf{y}} \right), \quad (70)$$

$$\underline{\boldsymbol{\zeta}}^{s(1)}(\underline{\mathbf{y}}) = \left( \frac{l_s}{l} \right)^2 \underline{\boldsymbol{\zeta}}^{s*} \left( \frac{l}{L} \underline{\mathbf{y}} \right), \quad \underline{\boldsymbol{\zeta}}^{a(1)}(\underline{\mathbf{y}}) = \left( \frac{l_a}{l} \right)^2 \underline{\boldsymbol{\zeta}}^{a*} \left( \frac{l}{L} \underline{\mathbf{y}} \right), \quad (71)$$

$$\underline{\boldsymbol{\zeta}}^{s(2)}(\underline{\mathbf{y}}) = \left( \frac{l_s}{L} \right)^2 \underline{\boldsymbol{\zeta}}^{s*} \left( \frac{l}{L} \underline{\mathbf{y}} \right), \quad \underline{\boldsymbol{\zeta}}^{a(2)}(\underline{\mathbf{y}}) = \left( \frac{l_a}{L} \right)^2 \underline{\boldsymbol{\zeta}}^{a*} \left( \frac{l}{L} \underline{\mathbf{y}} \right) \quad (72)$$

They are  $Y$ -periodic since  $\underline{\mathbf{a}}^*$ ,  $\underline{\mathbf{b}}^*$  and  $\underline{\mathbf{c}}^*$  are  $Y^*$ -periodic. Four different hypotheses will be made concerning the constitutive tensors of problem  $\mathcal{P}_\epsilon$  :

$$\text{Assumption 1: } \underline{\mathbf{a}}^\epsilon(\underline{\mathbf{x}}^*) = \underline{\mathbf{a}}^{(0)}(\epsilon^{-1}\underline{\mathbf{x}}^*), \underline{\mathbf{b}}^\epsilon(\underline{\mathbf{x}}^*) = \underline{\mathbf{b}}^{(0)}(\epsilon^{-1}\underline{\mathbf{x}}^*) \text{ and} \\ \underline{\mathbf{c}}^\epsilon(\underline{\mathbf{x}}^*) = \epsilon^2 \underline{\mathbf{c}}^{(1)}(\epsilon^{-1}\underline{\mathbf{x}}^*);$$

$$\text{Assumption 2: } \underline{\mathbf{a}}^\epsilon(\underline{\mathbf{x}}^*) = \underline{\mathbf{a}}^{(0)}(\epsilon^{-1}\underline{\mathbf{x}}^*), \underline{\mathbf{b}}^\epsilon(\underline{\mathbf{x}}^*) = \underline{\mathbf{b}}^{(0)}(\epsilon^{-1}\underline{\mathbf{x}}^*) \text{ and} \\ \underline{\mathbf{c}}^\epsilon(\underline{\mathbf{x}}^*) = \underline{\mathbf{c}}^{(2)}(\epsilon^{-1}\underline{\mathbf{x}}^*);$$

$$\text{Assumption 3: } \underline{\mathbf{a}}^\epsilon(\underline{\mathbf{x}}^*) = \underline{\mathbf{a}}^{(0)}(\epsilon^{-1}\underline{\mathbf{x}}^*), \underline{\mathbf{b}}^\epsilon(\underline{\mathbf{x}}^*) = \underline{\mathbf{b}}^{(0)}(\epsilon^{-1}\underline{\mathbf{x}}^*) \text{ and} \\ \underline{\mathbf{c}}^{s\epsilon}(\underline{\mathbf{x}}^*) = \epsilon^2 \underline{\mathbf{c}}^{s(1)}(\epsilon^{-1}\underline{\mathbf{x}}^*), \underline{\mathbf{c}}^{a\epsilon}(\underline{\mathbf{x}}^*) = \underline{\mathbf{c}}^{a(2)}(\epsilon^{-1}\underline{\mathbf{x}}^*);$$

$$\text{Assumption 4: } \underline{\mathbf{a}}^\epsilon(\underline{\mathbf{x}}^*) = \underline{\mathbf{a}}^{(0)}(\epsilon^{-1}\underline{\mathbf{x}}^*), \underline{\mathbf{b}}^\epsilon(\underline{\mathbf{x}}^*) = \underline{\mathbf{b}}^{(0)}(\epsilon^{-1}\underline{\mathbf{x}}^*) \text{ and} \\ \underline{\mathbf{c}}^{s\epsilon}(\underline{\mathbf{x}}^*) = \underline{\mathbf{c}}^{s(2)}(\epsilon^{-1}\underline{\mathbf{x}}^*), \underline{\mathbf{c}}^{a\epsilon}(\underline{\mathbf{x}}^*) = \epsilon^2 \underline{\mathbf{c}}^{a(1)}(\epsilon^{-1}\underline{\mathbf{x}}^*).$$

Assumptions 1 and 2 respectively correspond to the homogenisation schemes HS1 and HS2. Both choices meet the requirement that

$$\left(\epsilon = \frac{l}{L}\right) \Rightarrow \left(\underline{\mathbf{a}}^\epsilon = \underline{\mathbf{a}}^* \quad \text{and} \quad \underline{\mathbf{c}}^\epsilon = \left(\frac{l_s}{L}\right)^2 \underline{\mathbf{c}}^*\right)$$

Assumptions 3 and 4 respectively correspond to the homogenisation schemes HS3 and HS4. Both choices meet the requirement that

$$\left(\epsilon = \frac{l}{L}\right) \Rightarrow \left(\underline{\mathbf{a}}^\epsilon = \underline{\mathbf{a}}^*, \quad \underline{\mathbf{c}}^{s\epsilon} = \left(\frac{l_s}{L}\right)^2 \underline{\mathbf{c}}^{s*} \quad \text{and} \quad \underline{\mathbf{c}}^{a\epsilon} = \left(\frac{l_a}{L}\right)^2 \underline{\mathbf{c}}^{a*}\right)$$

It must be noted that, in our presentation of the asymptotic analysis, the lengths  $l, l_s, l_a$  and  $L$  are given and fixed, whereas parameter  $\epsilon$  is allowed to tend to zero in the limiting process.

In the sequel, the stars  $*$  are dropped for conciseness.

## Multiscale asymptotic method

In the setting of the homogenisation problems two space variables have been distinguished :  $\underline{\mathbf{x}}$  describes the macroscopic scale and  $\underline{\mathbf{y}}$  is the local variable in the unit cell  $Y$ . To solve the homogenisation problem, it is resorted to the method of multiscale asymptotic developments initially introduced in Sanchez-Palencia (1974). According to this method, all fields are regarded as functions of both variables  $\underline{\mathbf{x}}$  and  $\underline{\mathbf{y}}$ . It is assumed that they can be expanded in a series of powers of small parameter  $\epsilon$ . In particular, the

displacement, micro-deformation, force and double stress fields are supposed to take the form :

$$\begin{aligned}
\mathbf{u}^\epsilon(\mathbf{x}) &= \mathbf{u}_0(\mathbf{x}, \mathbf{y}) + \epsilon \mathbf{u}_1(\mathbf{x}, \mathbf{y}) + \epsilon^2 \mathbf{u}_2(\mathbf{x}, \mathbf{y}) + \dots \\
\mathbf{\chi}^\epsilon(\mathbf{x}) &= \mathbf{\chi}_1(\mathbf{x}, \mathbf{y}) + \epsilon \mathbf{\chi}_2(\mathbf{x}, \mathbf{y}) + \epsilon^2 \mathbf{\chi}_3(\mathbf{x}, \mathbf{y}) + \dots \\
\mathbf{\sigma}^\epsilon(\mathbf{x}) &= \mathbf{\sigma}_0(\mathbf{x}, \mathbf{y}) + \epsilon \mathbf{\sigma}_1(\mathbf{x}, \mathbf{y}) + \epsilon^2 \mathbf{\sigma}_2(\mathbf{x}, \mathbf{y}) + \dots \\
\mathbf{s}^\epsilon(\mathbf{x}) &= \mathbf{s}_0(\mathbf{x}, \mathbf{y}) + \epsilon \mathbf{s}_1(\mathbf{x}, \mathbf{y}) + \epsilon^2 \mathbf{s}_2(\mathbf{x}, \mathbf{y}) + \dots \\
\mathbf{m}^\epsilon(\mathbf{x}) &= \mathbf{m}_0(\mathbf{x}, \mathbf{y}) + \epsilon \mathbf{m}_1(\mathbf{x}, \mathbf{y}) + \epsilon^2 \mathbf{m}_2(\mathbf{x}, \mathbf{y}) + \dots
\end{aligned} \tag{73}$$

where the coefficients  $\mathbf{u}_i(\mathbf{x}, \mathbf{y})$ ,  $\mathbf{\chi}_i(\mathbf{x}, \mathbf{y})$ ,  $\mathbf{\sigma}_i(\mathbf{x}, \mathbf{y})$ ,  $\mathbf{s}_i(\mathbf{x}, \mathbf{y})$  and  $\mathbf{m}_i(\mathbf{x}, \mathbf{y})$  are assumed to have the same order of magnitude and to be  $Y$ -periodic with respect to variable  $\mathbf{y}$  ( $\mathbf{y} = \mathbf{x}/\epsilon$ ). The average operator over the unit cell  $Y$  is denoted by

$$\langle \cdot \rangle = \frac{1}{|Y|} \int_Y \cdot dV$$

As a result,

$$\langle \mathbf{u}^\epsilon \rangle = \mathbf{U}_0 + \epsilon \mathbf{U}_1 + \dots \quad \text{and} \quad \langle \mathbf{\chi}^\epsilon \rangle = \mathbf{\Xi}_1 + \epsilon \mathbf{\Xi}_2 + \dots \tag{74}$$

where  $\mathbf{U}_i = \langle \mathbf{u}_i \rangle$  and  $\mathbf{\Xi}_i = \langle \mathbf{\chi}_i \rangle$ . The gradient operator can be split into partial derivatives with respect to  $\mathbf{x}$  and  $\mathbf{y}$  :

$$\nabla = \nabla_x + \frac{1}{\epsilon} \nabla_y \tag{75}$$

This operator is used to compute the strain measures and balance equations :

$$\begin{aligned}
\mathbf{\xi}^\epsilon &= \epsilon^{-1} \mathbf{\xi}_{-1} + \mathbf{\xi}_0 + \epsilon^1 \mathbf{\xi}_1 + \dots \\
&= \epsilon^{-1} \mathbf{u}_0 \otimes^s \nabla_y + (\mathbf{u}_0 \otimes^s \nabla_x + \mathbf{u}_1 \otimes^s \nabla_y) \\
&\quad + \epsilon (\mathbf{u}_1 \otimes^s \nabla_x + \mathbf{u}_2 \otimes^s \nabla_y) + \dots \\
\mathbf{\xi}^\epsilon &= \epsilon^{-1} \mathbf{e}_{-1} + \mathbf{e}_0 + \epsilon^1 \mathbf{e}_1 + \dots \\
&= \epsilon^{-1} \mathbf{u}_0 \otimes \nabla_y + (\mathbf{u}_0 \otimes \nabla_x + \mathbf{u}_1 \otimes \nabla_y - \mathbf{\chi}_1) \\
&\quad + \epsilon (\mathbf{u}_1 \otimes \nabla_x + \mathbf{u}_2 \otimes \nabla_y - \mathbf{\chi}_2) + \dots \\
\mathbf{\kappa}^\epsilon &= \epsilon^{-1} \mathbf{\kappa}_{-1} + \mathbf{\kappa}_0 + \epsilon^1 \mathbf{\kappa}_1 + \dots \\
&= \epsilon^{-1} \mathbf{\chi}_1 \otimes \nabla_y + (\mathbf{\chi}_1 \otimes \nabla_x + \mathbf{\chi}_2 \otimes \nabla_y) \\
&\quad + \epsilon (\mathbf{\chi}_2 \otimes \nabla_x + \mathbf{\chi}_3 \otimes \nabla_y) + \dots
\end{aligned}$$

$$(\mathbf{\sigma}^\epsilon + \mathbf{s}^\epsilon) \cdot \nabla_x + \epsilon^{-1} (\mathbf{\sigma}^\epsilon + \mathbf{s}^\epsilon) \cdot \nabla_y = 0, \quad \mathbf{m}^\epsilon \cdot \nabla_x + \epsilon^{-1} \mathbf{m}^\epsilon \cdot \nabla_y + \mathbf{s}^\epsilon = 0 \tag{76}$$

Similar expansions are valid for the tensors  $\mathbf{\kappa}^s, \mathbf{\kappa}^a$ . The expansions of the stress tensors are then introduced in the balance equations (76) and the terms can be ordered with respect to the powers of  $\epsilon$ . Identifying the terms of same order, we are lead to the following set of equations :

- order  $\epsilon^{-1}$ ,

$$(\underline{\sigma}_0 + \underline{s}_0) \cdot \nabla_y = 0 \quad \text{and} \quad \underline{\underline{m}}_0 \cdot \nabla_y = 0 \quad (77)$$

- order  $\epsilon^0$ ,

$$(\underline{\sigma}_0 + \underline{s}_0) \cdot \nabla_x + (\underline{\sigma}_1 + \underline{s}_1) \cdot \nabla_y = 0 \quad \text{and} \quad \underline{\underline{S}}_0 \cdot \nabla_x + \underline{\underline{S}}_1 \cdot \nabla_y + \underline{s}_1 = 0 \quad (78)$$

The effective balance equations follow (78) by averaging over the unit cell  $Y$  and, at the order  $\epsilon^0$  one gets :

$$(\underline{\Sigma}_0 + \underline{\underline{S}}_0) \cdot \nabla = 0 \quad \text{and} \quad \underline{\underline{M}}_0 \cdot \nabla + \underline{\underline{S}}_0 = 0 \quad (79)$$

where  $\underline{\Sigma}_0 = \langle \underline{\sigma}_0 \rangle$ ,  $\underline{\underline{S}}_0 = \langle \underline{s}_0 \rangle$  and  $\underline{\underline{M}}_0 = \langle \underline{\underline{m}}_0 \rangle$ .

### Homogenization scheme HS1

For the first homogenisation scheme defined in section 4.1, the equations describing the local behaviour are :

$$\underline{\sigma}^\epsilon = \underline{\underline{a}}^{(0)}(\underline{y}) : \underline{\epsilon}^\epsilon, \quad \underline{s}^\epsilon = \underline{\underline{b}}^{(0)}(\underline{y}) : \underline{e}^\epsilon \quad \text{and} \quad \underline{\underline{m}}^\epsilon = \epsilon^2 \underline{\underline{c}}^{(1)}(\underline{y}) : \underline{\kappa}^\epsilon \quad (80)$$

At this stage, the expansion (76) can be substituted into the constitutive equations (80). Identifying the terms of same order, we get :

- order  $\epsilon^{-1}$ ,

$$\underline{\underline{a}}^{(0)} : \underline{\epsilon}_{-1} = \underline{\underline{a}}^{(0)} : (\underline{\underline{u}}_0 \overset{s}{\otimes} \nabla_y) = 0, \quad \underline{\underline{b}}^{(0)} : \underline{e}_0 = \underline{\underline{b}}^{(0)} : (\underline{\underline{u}}_0 \otimes \nabla_y) = 0 \quad (81)$$

- order  $\epsilon^0$ ,

$$\underline{\sigma}_0 = \underline{\underline{a}}^{(0)} : \underline{\epsilon}_0, \quad \underline{s}_0 = \underline{\underline{b}}^{(0)} : \underline{e}_0, \quad \underline{\underline{m}}_0 = 0 \quad (82)$$

- order  $\epsilon^1$ ,

$$\underline{\sigma}_1 = \underline{\underline{a}}^{(0)} : \underline{\epsilon}_1, \quad \underline{s}_1 = \underline{\underline{b}}^{(0)} : \underline{e}_1, \quad \underline{\underline{m}}_1 = \underline{\underline{c}}^{(1)} : \underline{\kappa}_{-1} \quad (83)$$

The equation (81) implies that  $\underline{\underline{u}}_0$  does not depend on the local variable  $\underline{y}$  :

$$\underline{\underline{u}}_0(\underline{x}, \underline{y}) = \underline{\underline{U}}_0(\underline{x})$$

At the order  $\epsilon^0$ , the higher order stress tensor vanishes,

$$\underline{\underline{M}}_0 = \langle \underline{\underline{m}}_0 \rangle = 0$$

Finally, the fields  $(\underline{\mathbf{u}}_1, \underline{\chi}_1, \underline{\boldsymbol{\sigma}}_0, \underline{\boldsymbol{\varepsilon}}_0, \underline{\mathbf{m}}_1)$  are solutions of the following auxiliary boundary value problem defined on the unit cell :

$$\begin{cases} \underline{\boldsymbol{\varepsilon}}_0 = \underline{\mathbf{U}}_0 \overset{s}{\otimes} \nabla_x + \underline{\mathbf{u}}_1 \overset{s}{\otimes} \nabla_y, & \underline{\boldsymbol{\varepsilon}}_0 = \underline{\mathbf{U}}_0 \otimes \nabla_x + \underline{\mathbf{u}}_1 \otimes \nabla_y - \underline{\chi}_1 \\ \underline{\boldsymbol{\kappa}}_{-1} = \underline{\chi}_1 \otimes \nabla_y \\ \underline{\boldsymbol{\sigma}}_0 = \underline{\mathbf{a}}^{(0)} : \underline{\boldsymbol{\varepsilon}}_0, & \underline{\boldsymbol{\varepsilon}}_0 = \underline{\mathbf{b}}^{(0)} : \underline{\boldsymbol{\varepsilon}}_0, & \underline{\mathbf{m}}_1 = \underline{\boldsymbol{\varepsilon}}_0^{(1)} : \underline{\boldsymbol{\kappa}}_{-1} \\ (\underline{\boldsymbol{\sigma}}_0 + \underline{\boldsymbol{\varepsilon}}_0) \cdot \nabla_y = 0, & \underline{\mathbf{m}}_1 \cdot \nabla_y + \underline{\boldsymbol{\varepsilon}}_0 = 0 \end{cases} \quad (84)$$

The boundary conditions of this problem are given by the periodicity requirements for the unknown fields. A series of auxiliary problems similar to (84) can be defined to obtain the solutions at higher orders. It must be noted that these problems must be solved in cascade since, for instance, the solution of (84) requires the knowledge of  $\underline{\mathbf{U}}_0$ . A particular solution  $\underline{\chi}$  for a vanishing prescribed  $\underline{\mathbf{U}}_0 \overset{s}{\otimes} \nabla_x$  is  $\underline{\chi} = \underline{\mathbf{U}}_0 \overset{a}{\otimes} \nabla_x$ . It follows that the solution  $(\underline{\mathbf{u}}_1, \underline{\mathbf{U}}_0 \overset{a}{\otimes} \nabla_x - \underline{\chi}_1)$  to problem (84) depends linearly on  $\underline{\mathbf{U}}_0 \overset{s}{\otimes} \nabla_x$ , up to a translation term, so that :

$$\underline{\mathbf{u}}^\epsilon = \underline{\mathbf{U}}_0(\underline{\mathbf{x}}) + \epsilon(\underline{\mathbf{U}}_1(\underline{\mathbf{x}}) + \underline{\mathbf{X}}_{\underline{u}}^{(1)}(\underline{\mathbf{y}}) : (\underline{\mathbf{U}}_0 \overset{s}{\otimes} \nabla)) + \dots \quad (85)$$

$$\underline{\chi}^\epsilon = \underline{\mathbf{U}}_0 \overset{a}{\otimes} \nabla_x + \underline{\mathbf{X}}_{\underline{\chi}}^{(1)}(\underline{\mathbf{y}}) : \underline{\mathbf{U}}_0 \overset{s}{\otimes} \nabla + \dots \quad (86)$$

where concentration tensors  $\underline{\mathbf{X}}_{\underline{u}}^{(1)}$  and  $\underline{\mathbf{X}}_{\underline{\chi}}^{(1)}$  have been introduced, the components of which are determined by the successive solutions of the auxiliary problem for unit values of the components of  $\underline{\mathbf{U}}_0 \overset{s}{\otimes} \nabla$ . Concentration tensor  $\underline{\mathbf{X}}_{\underline{u}}^{(1)}$  is such that its mean value over the unit cell vanishes.

The macroscopic stress tensor is given by :

$$\underline{\boldsymbol{\Sigma}}_0 = \langle \underline{\boldsymbol{\sigma}}_0 \rangle = \langle \underline{\mathbf{a}}^{(0)} : (\underline{\mathbf{1}} + \nabla_x \overset{s}{\otimes} \underline{\mathbf{X}}_{\underline{u}}^{(1)}) \rangle : (\underline{\mathbf{U}}_0 \overset{s}{\otimes} \nabla) = \underline{\mathbf{A}}_0^{(1)} : (\underline{\mathbf{U}}_0 \overset{s}{\otimes} \nabla) \quad (87)$$

Accordingly, the tensor of effective moduli possesses all symmetries of classical elastic moduli for a Cauchy medium :

$$A_{0ijkl}^{(1)} = A_{0klij}^{(1)} = A_{0jikl}^{(1)} = A_{0ijlk}^{(1)}$$

The additional second rank stress tensor can be shown to vanish :

$$\underline{\boldsymbol{S}}_0 = \langle \underline{\boldsymbol{\varepsilon}}_0 \rangle = \langle -\underline{\mathbf{m}}_1 \cdot \nabla_y \rangle = 0 \quad (88)$$

The effective medium is therefore governed by the single equation :

$$\underline{\underline{\Sigma}}_0 \cdot \nabla = 0 \quad (89)$$

The effective medium turns out to be a Cauchy continuum with symmetric stress tensor.

## Homogenization scheme HS2

For the second homogenisation scheme defined in section 4.1, the equations describing the local behaviour are :

$$\underline{\underline{\sigma}}^\epsilon = \underline{\underline{a}}^{(0)}(\underline{\underline{y}}) : \underline{\underline{\varepsilon}}^\epsilon, \quad \underline{\underline{s}}^\epsilon = \underline{\underline{b}}^{(0)}(\underline{\underline{y}}) : \underline{\underline{e}}^\epsilon, \quad \text{and} \quad \underline{\underline{m}}^\epsilon = \underline{\underline{c}}^{(2)}(\underline{\underline{y}}) : \underline{\underline{\kappa}}^\epsilon \quad (90)$$

The different steps of the asymptotic analysis are the same as in the previous section for HS1. We will only focus here on the main results. At the order  $\epsilon^{-1}$ , one gets

$$\underline{\underline{a}}^{(0)} : \underline{\underline{\varepsilon}}_{-1} = 0, \quad \underline{\underline{b}}^{(0)} : \underline{\underline{e}}_{-1} = 0, \quad \underline{\underline{c}}^{(2)} : \underline{\underline{\kappa}}_{-1} = 0 \quad (91)$$

This implies that the gradients of  $\underline{\underline{u}}_0$  and  $\underline{\underline{\chi}}_1$  with respect to  $\underline{\underline{y}}$  vanish, so that :

$$\underline{\underline{u}}_0(\underline{\underline{x}}, \underline{\underline{y}}) = \underline{\underline{U}}_0(\underline{\underline{x}}), \quad \underline{\underline{\chi}}_1(\underline{\underline{x}}, \underline{\underline{y}}) = \underline{\underline{\Xi}}_1(\underline{\underline{x}}) \quad (92)$$

The fields  $(\underline{\underline{u}}_1, \underline{\underline{\chi}}_1, \underline{\underline{\sigma}}_0, \underline{\underline{s}}_0, \underline{\underline{m}}_0)$  are solutions of the two following auxiliary boundary value problems defined on the unit cell :

$$\begin{cases} \underline{\underline{\varepsilon}}_0 = \underline{\underline{U}}_0 \overset{s}{\otimes} \nabla_x + \underline{\underline{u}}_1 \overset{s}{\otimes} \nabla_y, & \underline{\underline{e}}_0 = \underline{\underline{U}}_0 \otimes \nabla_x + \underline{\underline{u}}_1 \otimes \nabla_y - \underline{\underline{\Xi}}_1 \\ \underline{\underline{\sigma}}_0 = \underline{\underline{a}}^{(0)} : \underline{\underline{\varepsilon}}_0, & \underline{\underline{s}}_0 = \underline{\underline{b}}^{(0)} : \underline{\underline{e}}_0 \\ (\underline{\underline{\sigma}}_0 + \underline{\underline{s}}_0) \cdot \nabla_y = 0 \end{cases}$$

$$\begin{cases} \underline{\underline{\kappa}}_0 = \underline{\underline{\Xi}}_1 \otimes \nabla_x + \underline{\underline{\chi}}_2 \otimes \nabla_y \\ \underline{\underline{m}}_0 = \underline{\underline{c}}^{(2)} : \underline{\underline{\kappa}}_0, & \underline{\underline{m}}_0 \cdot \nabla_y = 0 \end{cases}$$

We are therefore left with two decoupled boundary value problems : the first one with main unknown  $\underline{\underline{u}}_1$  depends linearly on  $\underline{\underline{U}}_0 \overset{s}{\otimes} \nabla_x$  and  $\underline{\underline{U}}_0 \otimes \nabla_x - \underline{\underline{\Xi}}_1$ , whereas the second one with unknown  $\underline{\underline{\chi}}_2$  is linear in  $\underline{\underline{\Xi}}_1 \otimes \nabla_x$ . The solutions take the form :

$$\begin{aligned} \underline{\underline{u}}^\epsilon &= \underline{\underline{U}}_0(\underline{\underline{x}}) + \epsilon(\underline{\underline{U}}_1(\underline{\underline{x}}) + \underline{\underline{X}}_u^{(2)}(\underline{\underline{y}}) : (\underline{\underline{U}}_0 \overset{s}{\otimes} \nabla) + \underline{\underline{X}}_e^{(2)}(\underline{\underline{y}}) : (\underline{\underline{U}}_0 \otimes \nabla - \underline{\underline{\Xi}}_1)) \\ &+ \dots, \quad \underline{\underline{\chi}}^\epsilon = \underline{\underline{\Xi}}_1(\underline{\underline{x}}) + \epsilon(\underline{\underline{\Xi}}_2(\underline{\underline{x}}) + \underline{\underline{X}}_\kappa^{(2)}(\underline{\underline{y}}) : (\underline{\underline{\Xi}}_1 \otimes \nabla)) + \dots \end{aligned} \quad (93)$$

where concentration tensors  $\underline{\underline{X}}_u^{(2)}$ ,  $\underline{\underline{X}}_e^{(2)}$  and  $\underline{\underline{X}}_\kappa^{(1)}$  have been introduced. Their components are determined by the successive solutions of the auxiliary problem for unit values of the components of  $\underline{\underline{U}}_0 \otimes \nabla$ ,  $\underline{\underline{U}}_0 \otimes \nabla - \underline{\underline{\Xi}}_1$  and  $\underline{\underline{\Xi}}_1 \otimes \nabla_y$ . They are such that their mean value over the unit cell vanishes.

The macroscopic stress tensors and effective elastic properties are given by :

$$\begin{aligned} \underline{\underline{\Sigma}}_0 &= \langle \underline{\underline{a}}^{(0)} : (\underline{\underline{1}} + \nabla_y \otimes \underline{\underline{X}}_u^{(2)}) \rangle : (\underline{\underline{U}}_0 \otimes \nabla) \\ &+ \langle \underline{\underline{a}}^{(0)} : (\nabla_y \otimes \underline{\underline{X}}_e^{(2)}) \rangle : (\underline{\underline{U}}_0 \otimes \nabla - \underline{\underline{\Xi}}_1) \end{aligned} \quad (94)$$

$$\begin{aligned} \underline{\underline{\mathcal{S}}}_0 &= \langle \underline{\underline{s}}_0 \rangle = \langle \underline{\underline{b}}^{(0)} : (\nabla_y \otimes \underline{\underline{X}}_u^{(2)}) \rangle : (\underline{\underline{U}}_0 \otimes \nabla) \\ &+ \langle \underline{\underline{b}}^{(0)} : (\nabla_y \otimes \underline{\underline{X}}_e^{(2)}) \rangle : (\underline{\underline{U}}_0 \otimes \nabla - \underline{\underline{\Xi}}_1) \end{aligned} \quad (95)$$

$$\underline{\underline{\mathcal{M}}}_0 = \langle \underline{\underline{m}}_0 \rangle = \langle \underline{\underline{c}}^{(2)} : (\underline{\underline{1}} + \nabla_y \otimes \underline{\underline{X}}_\kappa^{(2)}) \rangle : \underline{\underline{\Xi}}_1 \otimes \nabla \quad (96)$$

None of these tensors vanishes in general, which means that the effective medium is a full micromorphic continuum governed by the balance equations (79).

### Homogenization scheme HS3

For the third homogenisation scheme defined in section 4.1, the equations describing the local behaviour are :

$$\underline{\underline{\sigma}}^\epsilon = \underline{\underline{a}}^{(0)}(\underline{\underline{y}}) : \underline{\underline{\varepsilon}}^\epsilon, \quad \underline{\underline{s}}^\epsilon = \underline{\underline{b}}^{(0)}(\underline{\underline{y}}) : \underline{\underline{e}}^\epsilon, \quad (97)$$

$$\underline{\underline{m}}^\epsilon = \epsilon^2 \underline{\underline{c}}^{s(1)}(\underline{\underline{y}}) : \underline{\underline{\kappa}}^{s\epsilon} + \underline{\underline{c}}^{a(2)}(\underline{\underline{y}}) : \underline{\underline{\kappa}}^{a\epsilon} \quad (98)$$

At the order  $\epsilon^{-1}$ , one gets

$$\underline{\underline{a}}^{(0)} : \underline{\underline{\varepsilon}}_{-1} = 0, \quad \underline{\underline{b}}^{(0)} : \underline{\underline{e}}_{-1} = 0, \quad \underline{\underline{c}}^{a(2)} : \underline{\underline{\kappa}}_{-1}^a = 0 \quad (99)$$

This implies that the gradients of  $\underline{\underline{u}}_0$  and  $\underline{\underline{\chi}}_1^a$  with respect to  $\underline{\underline{y}}$  vanish, so that :

$$\underline{\underline{u}}_0(\underline{\underline{x}}, \underline{\underline{y}}) = \underline{\underline{U}}_0(\underline{\underline{x}}), \quad \underline{\underline{\chi}}_1^a(\underline{\underline{x}}, \underline{\underline{y}}) = \underline{\underline{\Xi}}_1^a(\underline{\underline{x}}) \quad (100)$$

The fields  $(\underline{\mathbf{u}}_1, \underline{\chi}_1^s, \underline{\chi}_2^a, \underline{\chi}_3^a, \underline{\boldsymbol{\sigma}}_0, \underline{\boldsymbol{\xi}}_0, \underline{\mathbf{m}}_0, \underline{\mathbf{m}}_1)$  are solutions of the following auxiliary boundary value problem defined on the unit cell :

$$\left\{ \begin{array}{l} \underline{\boldsymbol{\varepsilon}}_0 = \underline{\mathbf{U}}_0 \overset{s}{\otimes} \nabla_x + \underline{\mathbf{u}}_1 \overset{s}{\otimes} \nabla_y, \quad \underline{\boldsymbol{\varepsilon}}_0 = \underline{\mathbf{U}}_0 \otimes \nabla_x + \underline{\mathbf{u}}_1 \otimes \nabla_y - \underline{\boldsymbol{\Xi}}_1^a - \underline{\chi}_1^s \\ \underline{\boldsymbol{\kappa}}_{-1}^s = \underline{\chi}_1^s \otimes \nabla_y, \quad \underline{\boldsymbol{\kappa}}_0^a = \underline{\boldsymbol{\Xi}}_1^a \otimes \nabla_x + \underline{\chi}_2^a \otimes \nabla_y, \quad \underline{\boldsymbol{\kappa}}_1^a = \underline{\chi}_2^a \otimes \nabla_x + \underline{\chi}_3^a \otimes \nabla_y \\ \underline{\boldsymbol{\sigma}}_0 = \underline{\mathbf{a}}^{(0)} : \underline{\boldsymbol{\varepsilon}}_0, \quad \underline{\boldsymbol{\xi}}_0 = \underline{\mathbf{b}}^{(0)} : \underline{\boldsymbol{\varepsilon}}_0 \\ \underline{\mathbf{m}}_0 = \underline{\mathbf{c}}^{a(2)} : \underline{\boldsymbol{\kappa}}_0^a, \quad \underline{\mathbf{m}}_1 = \underline{\mathbf{c}}^{s(1)} : \underline{\boldsymbol{\kappa}}_{-1}^s + \underline{\mathbf{c}}^{a(2)} : \underline{\boldsymbol{\kappa}}_1^a \\ (\underline{\boldsymbol{\sigma}}_0 + \underline{\boldsymbol{\xi}}_0) \cdot \nabla_y = 0, \quad \underline{\mathbf{m}}_0 \cdot \nabla_y = 0, \quad \underline{\mathbf{m}}_0 \cdot \nabla_x + \underline{\mathbf{m}}_1 \cdot \nabla_y + \underline{\boldsymbol{\xi}}_0 = 0 \end{array} \right.$$

This complex problem can be seen to depend linearly on  $\underline{\mathbf{U}}_0 \overset{s}{\otimes} \nabla, \underline{\mathbf{U}}_0 \overset{a}{\otimes} \nabla - \underline{\boldsymbol{\Xi}}_1^a$  and  $\underline{\boldsymbol{\Xi}}_1^a \otimes \nabla$ . The solutions take the form :

$$\begin{aligned} \underline{\mathbf{u}}^\epsilon &= \underline{\mathbf{U}}_0(\underline{\mathbf{x}}) + \epsilon(\underline{\mathbf{U}}_1(\underline{\mathbf{x}}) + \underline{\mathbf{X}}_u^{(3)}(\underline{\mathbf{y}})) : (\underline{\mathbf{U}}_0 \overset{s}{\otimes} \nabla) \\ &+ \underline{\mathbf{X}}_e^{(3)}(\underline{\mathbf{y}}) : (\underline{\mathbf{U}}_0 \overset{a}{\otimes} \nabla - \underline{\boldsymbol{\Xi}}_1^a) + \dots \end{aligned} \quad (101)$$

$$\underline{\boldsymbol{\chi}}^\epsilon = \underline{\boldsymbol{\Xi}}_1(\underline{\mathbf{x}}) + \epsilon(\underline{\boldsymbol{\Xi}}_2(\underline{\mathbf{x}}) + \underline{\mathbf{X}}_\kappa^{(3)}(\underline{\mathbf{y}})) : (\underline{\boldsymbol{\Xi}}_1^a \otimes \nabla) + \dots \quad (102)$$

where concentration tensors  $\underline{\mathbf{X}}_u^{(3)}, \underline{\mathbf{X}}_e^{(3)}$  and  $\underline{\mathbf{X}}_\kappa^{(3)}$  have been introduced. Their components are determined by the successive solutions of the auxiliary problem for unit values of the components of  $\underline{\mathbf{U}}_0 \overset{s}{\otimes} \nabla, \underline{\mathbf{U}}_0 \overset{a}{\otimes} \nabla - \underline{\boldsymbol{\Xi}}_1^a$  and  $\underline{\boldsymbol{\Xi}}_1^a \otimes \nabla_y$ . They are such that their mean value over the unit cell vanishes.

The macroscopic stress tensors and effective elastic properties are given by :

$$\begin{aligned} \underline{\boldsymbol{\Sigma}}_0 &= \langle \underline{\mathbf{a}}^{(0)} : (\underline{\mathbf{1}} + \nabla_x \otimes \underline{\mathbf{X}}_u^{(3)}) \rangle : (\underline{\mathbf{U}}_0 \overset{s}{\otimes} \nabla) \\ &+ \langle \underline{\mathbf{a}}^{(0)} : (\nabla_y \otimes \underline{\mathbf{X}}_e^{(3)}) \rangle : (\underline{\mathbf{U}}_0 \overset{a}{\otimes} \nabla - \underline{\boldsymbol{\Xi}}_1^a) \end{aligned} \quad (103)$$

$$\begin{aligned} \underline{\boldsymbol{\mathcal{S}}}_0 &= \langle \underline{\mathbf{s}}_0 \rangle = \langle \underline{\mathbf{b}}^{(0)} : (\nabla_y \otimes \underline{\mathbf{X}}_u^{(3)}) \rangle : (\underline{\mathbf{U}}_0 \overset{s}{\otimes} \nabla) \\ &+ \langle \underline{\mathbf{b}}^{(0)} : (\nabla_y \otimes \underline{\mathbf{X}}_e^{(3)}) \rangle : (\underline{\mathbf{U}}_0 \overset{a}{\otimes} \nabla - \underline{\boldsymbol{\Xi}}_1^a) \end{aligned} \quad (104)$$

$$\underline{\mathbf{M}}_0 = \langle \underline{\mathbf{m}}_0 \rangle = \langle \underline{\mathbf{c}}^{a(2)} : (\underline{\mathbf{1}} + \nabla_y \otimes \underline{\mathbf{X}}_\kappa^{(3)}) \rangle : \underline{\boldsymbol{\Xi}}_1^a \otimes \nabla \quad (105)$$

They must fulfill the balance equations (79). Note that  $\underline{\mathbf{m}}_0$  and therefore  $\underline{\mathbf{M}}_0$  are skew-symmetric with respect to their first two indices. The averaged equation of balance of moment of momentum implies then that  $\underline{\boldsymbol{\mathcal{S}}}_0$  is

skew-symmetric. The macroscopic degrees of freedom are the displacement field  $\underline{\mathbf{U}}_0$  and the rotation associated to  $\underline{\Xi}_1^a$ . The found balance and constitutive equations are therefore that of a Cosserat effective medium. The more classical form of the Cosserat theory is retrieved once one rewrites the previous equations using the axial vector associated to  $\underline{\Xi}^a$  (Forest, 2001).

#### Homogenization scheme HS4

For the last homogenisation scheme defined in section 4.1, the equations describing the local behaviour are :

$$\underline{\boldsymbol{\sigma}}^\epsilon = \underline{\mathbf{a}}^{(0)}(\underline{\mathbf{y}}) : \underline{\boldsymbol{\varepsilon}}^\epsilon, \quad \underline{\boldsymbol{s}}^\epsilon = \underline{\mathbf{b}}^{(0)}(\underline{\mathbf{y}}) : \underline{\boldsymbol{e}}^\epsilon \quad (106)$$

$$\underline{\mathbf{m}}^\epsilon = \underline{\underline{\mathbf{c}}}^{s(2)}(\underline{\mathbf{y}}) : \underline{\underline{\boldsymbol{\kappa}}}^{s\epsilon} + \epsilon^2 \underline{\underline{\mathbf{c}}}^{a(1)}(\underline{\mathbf{y}}) : \underline{\underline{\boldsymbol{\kappa}}}^{a\epsilon} \quad (107)$$

At the order  $\epsilon^{-1}$ , one gets

$$\underline{\mathbf{a}}^{(0)} : \underline{\boldsymbol{\varepsilon}}_{-1} = 0, \quad \underline{\mathbf{b}}^{(0)} : \underline{\boldsymbol{e}}_{-1} = 0, \quad \underline{\underline{\mathbf{c}}}^{s(2)} : \underline{\underline{\boldsymbol{\kappa}}}^s_{-1} = 0 \quad (108)$$

This implies that the gradients of  $\underline{\mathbf{u}}_0$  and  $\underline{\chi}_1^s$  with respect to  $\underline{\mathbf{y}}$  vanish, so that :

$$\underline{\mathbf{u}}_0(\underline{\mathbf{x}}, \underline{\mathbf{y}}) = \underline{\mathbf{U}}_0(\underline{\mathbf{x}}), \quad \underline{\chi}_1^s(\underline{\mathbf{x}}, \underline{\mathbf{y}}) = \underline{\Xi}_1^s(\underline{\mathbf{x}}) \quad (109)$$

The fields  $(\underline{\mathbf{u}}_1, \underline{\chi}_1^a, \underline{\chi}_2^s, \underline{\chi}_3^s, \underline{\boldsymbol{\sigma}}_0, \underline{\boldsymbol{s}}_0, \underline{\mathbf{m}}_0, \underline{\mathbf{m}}_1)$  are solutions of the following auxiliary boundary value problem defined on the unit cell :

$$\left\{ \begin{array}{l} \underline{\boldsymbol{\varepsilon}}_0 = \underline{\mathbf{U}}_0 \overset{s}{\otimes} \nabla_x + \underline{\mathbf{u}}_1 \overset{s}{\otimes} \nabla_y, \quad \underline{\boldsymbol{e}}_0 = \underline{\mathbf{U}}_0 \otimes \nabla_x + \underline{\mathbf{u}}_1 \otimes \nabla_y - \underline{\Xi}_1^s - \underline{\chi}_1^a \\ \underline{\underline{\boldsymbol{\kappa}}}^a_{-1} = \underline{\chi}_1^a \otimes \nabla_y, \quad \underline{\underline{\boldsymbol{\kappa}}}^s_0 = \underline{\Xi}_1^s \otimes \nabla_x + \underline{\chi}_2^s \otimes \nabla_y, \quad \underline{\underline{\boldsymbol{\kappa}}}^a_1 = \underline{\chi}_2^a \otimes \nabla_x + \underline{\chi}_3^a \otimes \nabla_y \\ \underline{\boldsymbol{\sigma}}_0 = \underline{\mathbf{a}}^{(0)} : \underline{\boldsymbol{\varepsilon}}_0, \quad \underline{\boldsymbol{s}}_0 = \underline{\mathbf{b}}^{(0)} : \underline{\boldsymbol{e}}_0 \\ \underline{\mathbf{m}}_0 = \underline{\underline{\mathbf{c}}}^{s(2)} : \underline{\underline{\boldsymbol{\kappa}}}^s_0, \quad \underline{\mathbf{m}}_1 = \underline{\underline{\mathbf{c}}}^{a(1)} : \underline{\underline{\boldsymbol{\kappa}}}^a_{-1} + \underline{\underline{\mathbf{c}}}^{s(2)} : \underline{\underline{\boldsymbol{\kappa}}}^s_1 \\ (\underline{\boldsymbol{\sigma}}_0 + \underline{\boldsymbol{s}}_0) \cdot \nabla_y = 0, \quad \underline{\mathbf{m}}_0 \cdot \nabla_y = 0, \quad \underline{\mathbf{m}}_0 \cdot \nabla_x + \underline{\mathbf{m}}_1 \cdot \nabla_y + \underline{\boldsymbol{s}}_0 = 0 \end{array} \right.$$

This complex problem can be seen to depend linearly on

$\underline{\mathbf{U}}_0 \overset{s}{\otimes} \nabla, \underline{\mathbf{U}}_0 \overset{s}{\otimes} \nabla - \underline{\Xi}_1^s$  and  $\underline{\Xi}_1^s \otimes \nabla$ . The solutions take the form :

$$\begin{aligned} \underline{\mathbf{u}}^\epsilon &= \underline{\mathbf{U}}_0(\underline{\mathbf{x}}) + \epsilon(\underline{\mathbf{U}}_1(\underline{\mathbf{x}}) + \underline{\mathbf{X}}_u^{(4)}(\underline{\mathbf{y}}) : (\underline{\mathbf{U}}_0 \overset{s}{\otimes} \nabla)) \\ &+ \underline{\mathbf{X}}_e^{(4)}(\underline{\mathbf{y}}) : (\underline{\mathbf{U}}_0 \overset{s}{\otimes} \nabla - \underline{\Xi}_1^s) + \dots \end{aligned} \quad (110)$$

$$\underline{\chi}^\epsilon = \underline{\Xi}_1(\underline{\mathbf{x}}) + \epsilon(\underline{\Xi}_2(\underline{\mathbf{x}}) + \underline{\mathbf{X}}_\kappa^{(4)}(\underline{\mathbf{y}}) : (\underline{\Xi}_1^s \otimes \nabla)) + \dots \quad (111)$$

where concentration tensors  $\underline{\underline{X}}_u^{(4)}$ ,  $\underline{\underline{X}}_e^{(4)}$  and  $\underline{\underline{X}}_\kappa^{(4)}$  have been introduced. Their components are determined by the successive solutions of the auxiliary problem for unit values of the components of  $\underline{\underline{U}}_0 \otimes \nabla$ ,  $\underline{\underline{U}}_0 \otimes \nabla - \underline{\underline{\Xi}}_1^s$  and  $\underline{\underline{\Xi}}_1^s \otimes \nabla_y$ . They are such that their mean value over the unit cell vanishes.

The macroscopic stress tensors and effective elastic properties are given by :

$$\begin{aligned} \underline{\underline{\Sigma}}_0 &= \langle \underline{\underline{a}}^{(0)} : (\underline{\underline{1}} + \nabla_x \otimes \underline{\underline{X}}_u^{(4)}) \rangle : (\underline{\underline{U}}_0 \otimes \nabla) \\ &+ \langle \underline{\underline{a}}^{(0)} : (\nabla_y \otimes \underline{\underline{X}}_e^{(4)}) \rangle : (\underline{\underline{U}}_0 \otimes \nabla - \underline{\underline{\Xi}}_1^s) \end{aligned} \quad (112)$$

$$\begin{aligned} \underline{\underline{S}}_0 = \langle \underline{\underline{s}}_0 \rangle &= \langle \underline{\underline{b}}^{(0)} : (\nabla_y \otimes \underline{\underline{X}}_u^{(4)}) \rangle : (\underline{\underline{U}}_0 \otimes \nabla) \\ &+ \langle \underline{\underline{b}}^{(0)} \rangle : (\underline{\underline{U}}_0 \otimes \nabla - \underline{\underline{\Xi}}_1^s) \end{aligned} \quad (113)$$

$$\underline{\underline{M}}_0 = \langle \underline{\underline{m}}_0 \rangle = \langle \underline{\underline{c}}^{s(2)} : (\underline{\underline{1}} + \nabla_y \otimes \underline{\underline{X}}_\kappa^{(4)}) \rangle : (\underline{\underline{\Xi}}_1^s \otimes \nabla) \quad (114)$$

They must fulfill the balance equations (79). Note that  $\underline{\underline{m}}_0$  and therefore  $\underline{\underline{M}}_0$  are symmetric with respect to their first two indices. The averaged equation of balance of moment of momentum implies then that  $\underline{\underline{S}}_0 = - \langle \underline{\underline{m}}_0 \rangle \cdot \nabla$  is symmetric. The macroscopic degrees of freedom are the displacement field  $\underline{\underline{U}}_0$  and the symmetric strain tensor  $\underline{\underline{\Xi}}_1^s$ . Such a continuum is called a microstrain medium (Forest and Sievert, 2006).

As a conclusion, depending on the relative contributions of the various intrinsic length scales of the micromorphic continuum, different effective media are obtained, as summarised in table 5. The effective medium can be of micromorphic, microstrain, Cosserat or Cauchy type.

homogenisation scheme	characteristic lengths	effective medium
HS1	$l_s \sim l, l_a \sim l$	Cauchy
HS2	$l_s \sim L, l_a \sim L$	micromorphic
HS3	$l_s \sim l, l_a \sim L$	Cosserat
HS4	$l_s \sim L, l_a \sim l$	microstrain

**Table 5.** Homogenization of heterogenous micromorphic media : Nature of the homogeneous equivalent medium depending on the values of the intrinsic lengths of the constituents.

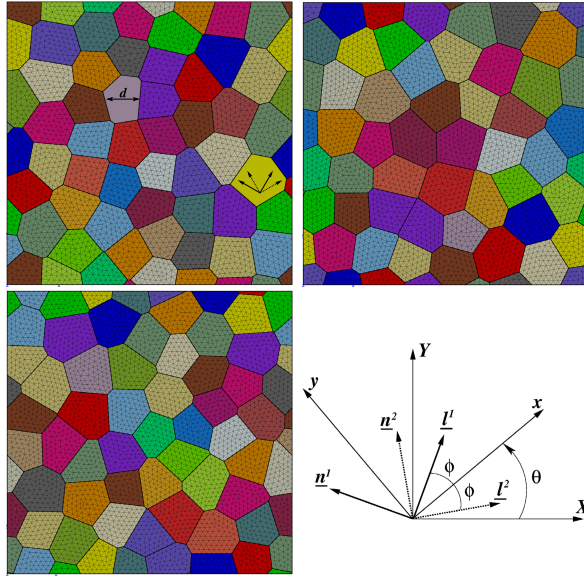


**Figure 10.** Periodic meshes of the 2D periodic aggregates used in the finite element simulations: (a) 52 grains, (b) 47 grains and (c) 55 grains. Two slip systems are taken into account in each randomly oriented grain. Various mean grain sizes,  $d$ , ranging from tens of nanometers to hundreds of microns, are investigated. (d) Description of the two effective slip systems for 2D planar double slip.

## 4.2 Application to polycrystalline plasticity

The previous homogenisation method is extended to non linear micromorphic constitutive equations in order to predict size effects in the plasticity of polycrystals. The micromorphic single crystal model is not presented here and the reader is referred to (Cordero et al., 2010, 2012) for a detailed presentation of the model and a more complete description of polycrystal homogenisation.

### Periodic homogenisation of micromorphic polycrystals

The computation of polycrystalline aggregates based on standard crystal plasticity models follows the rule of classical homogenisation theory in the sense that a mean strain is prescribed to a volume element of poly-

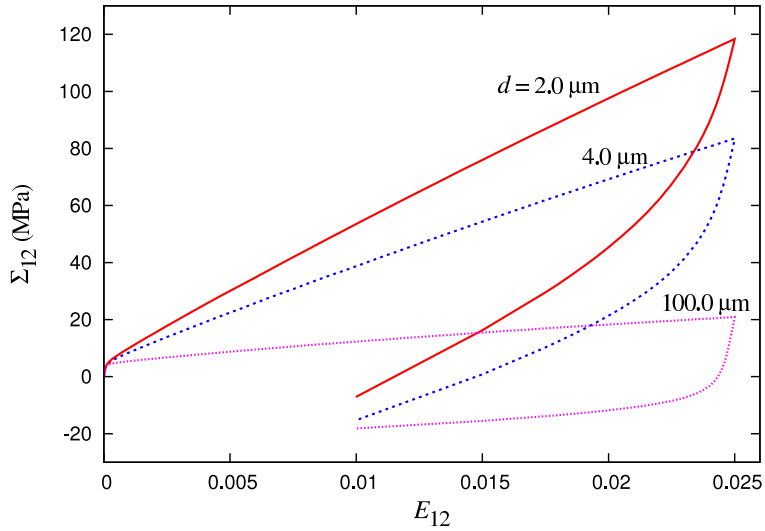


**Figure 11.** Macroscopic stress–strain response of the 52–grain aggregate of Fig. 10(a) under simple shear loading conditions including unloading for three different grain sizes.

crystalline materials using suitable boundary conditions like strain–based, stress–based or periodic ones. The structure of the boundary value problem is modified if a generalized continuum approach is used inside the considered volume element. In the present work, we are considering the computational homogenisation of a heterogeneous micromorphic medium and suitable boundary conditions for displacement and plastic microdeformation must be defined. In the case of linear material behavior, the structure of the unit cell problem to be solved can be derived from multiscale asymptotic expansion analysis, as shown in section 4.1. The obtained boundary conditions are then assumed to hold also for non–linear material responses. We look for the displacement field  $\underline{\mathbf{u}}$  and the plastic microdeformation field  $\underline{\underline{\chi}}^p$  in the polycrystal volume element such that

$$\underline{\mathbf{u}}(\underline{\mathbf{x}}) = \underline{\underline{\mathbf{E}}} \cdot \underline{\mathbf{x}} + \underline{\mathbf{v}}(\underline{\mathbf{x}}), \quad \forall \underline{\mathbf{x}} \in V \quad (115)$$

the fluctuation  $\underline{\mathbf{v}}$  being periodic at homologous points of the boundary  $\partial V$ . Under these conditions the prescribed average strain is the symmetric second order tensor  $\underline{\underline{\mathbf{E}}}$ . The plastic microdeformation  $\underline{\underline{\chi}}^p$  is periodic at ho-

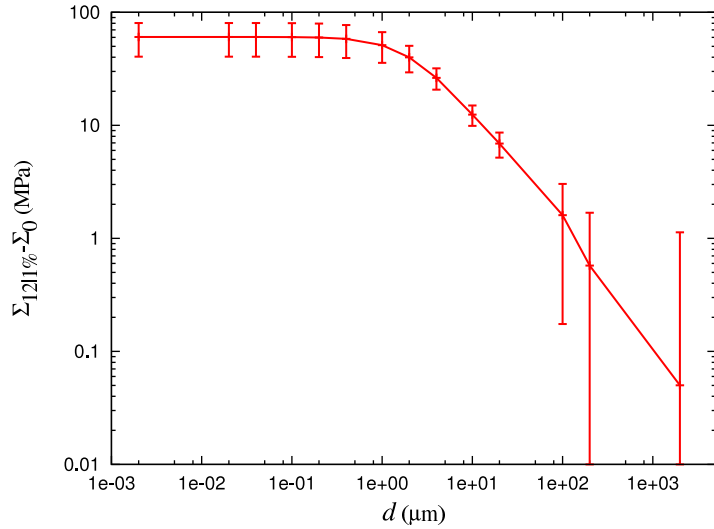


**Figure 12.** Effect of the mean grain size,  $d$ , on the macroscopic flow stress  $\Sigma_{12|1\%}$  at 1% mean plastic strain. The results are obtained with the three aggregates of Fig. 10 under simple shear. The error bars give the standard deviation.

mologous points of  $\partial V$ . As a result, the mean value of the microdeformation gradient  $\tilde{\Gamma}$  vanishes.

The grain boundary conditions must now be discussed. At any interface of a micromorphic continuum, there may exist some jump conditions for the degrees of freedom of the theory and the associated reactions, namely the simple and double traction vectors. We consider in this work that such jumps do not exist. Instead, the displacement vector and the plastic microdeformation tensor are assumed to be continuous at grain boundaries. As a result, the simple and double tractions also are continuous. The continuity of plastic microdeformation is a new grain boundary condition that does not exist in classical crystal plasticity. It will generate boundary layers at grain boundaries which are essential for the observed size effects (Cordero et al., 2010). Let us imagine a grain boundary between a plastically deforming grain and an elastic grain where plasticity is not triggered. The condition of continuity of plastic microdeformation implies that the plastic microdeformation should vanish at this grain boundary, thus leading to a decrease of plastic slip close to the grain boundary, associated with pile-up forma-

tion. More generally continuity of plastic microdeformation is enforced at grain boundaries. Also grain boundaries are assumed to transmit simple and double tractions. Jump conditions or more specific interface laws may well be more realistic or physically motivated but they would require additional considerable computational effort. We think that the continuity conditions carry the main physical ingredient to capture the targeted size effects in plasticity.

The simulations are limited to two-dimensional crystals under plane strain conditions and a mean shear strain  $E_{12}$  is prescribed to the volume elements. Three volume elements are considered, made of 52, 47 and 55 grains, respectively, according to a 2D Voronoi tessellation with periodic constraints. They are shown in Fig. 10. The three realisations of the material have different grain shapes and different orientations chosen randomly. Homothetic volumes constructed from the three previous volume elements will be considered, thus having different mean grain sizes but the same grain morphology and crystallographic texture.

Only two planar slip systems are considered in most simulations of this work. The slip directions and normal to the slip planes are contained in the considered plane. They are separated by the angle  $2\phi$  with  $\phi = 35.1^\circ$  following Bennett and McDowell (2003). The sets of material parameters used for the simulations are given in (Cordero et al., 2012).

The micromorphic constitutive model contains a characteristic length equal here to  $l_w = 450$  nm. Note that this intrinsic length is defined from the ratio of two constitutive moduli for reason of dimensionality. The resulting characteristic thickness of boundary layers affected by the strain gradient effects, especially close to grain boundary, will generally be proportional to  $l_w$  with a factor depending on other constitutive parameters and on the type of boundary value problem. Such characteristic lengths have been derived from analytical solutions in some simple boundary value problems in (Cordero et al., 2010). For polycrystals, they will emerge from the computational analysis.

### **Evidence of size-dependent kinematic hardening**

Fig. 11 gives the mean shear stress as a function of mean shear strain as a result of a finite element simulation of the 52-grain aggregate of Fig. 10(a) for three different grain sizes. One shear loading branch up to 0.025 mean shear strain followed by the unloading branch are presented. The stress-strain curves clearly exhibit an overall kinematic hardening effect induced by the local contributions of the double stress tensor, as proved in (Cordero et al., 2010). The kinematic hardening vanishes for large grains and is all the stronger as the grain size is smaller.

From the overall shear curves, the shear stress value  $\Sigma_{12|p_0}$  was recorded at a given level of mean plastic microstrain  $\chi_{12}^{ps} = p_0$  where  $\chi_{12}^{ps}$  is defined as:

$$\chi_{12}^{ps} = (\chi_{12}^p + \chi_{21}^p)/2 \quad (116)$$

The mean shear stress  $\Sigma_{12|p_0}$  was plotted as a function of grain size. It turns out that the shear stress value converges toward a fixed value  $\Sigma_0$  for large grain sizes. This limit depends only on the value of the critical resolved shear stress entering the Schmid law and on the specific geometry and orientations of the considered polycrystalline aggregates. It is therefore possible to draw a Hall–Petch diagram which is a log–log plot of  $\Sigma_{12|p_0} - \Sigma_0$  vs. the grain size  $d$ . Such a plot is given in Fig. 12 for  $p_0 = 0.01$ . The continuous line gives the mean value of the shear stress level for the three realizations of the microstructure considered in Fig. 10. Error bars are also provided showing the scatter of the results which is rather strong due to the small number of grains in each microstructure and the small number of considered aggregates. The diagram of Fig. 12 clearly shows two regimes in the relation between stress level and grain size. For grain sizes smaller than  $1 \mu\text{m}$ , no dependence of the overall stress on grain size is observed. For grain sizes larger than  $1 \mu\text{m}$ , a power law is found in the form

$$\Sigma_{12|p_0} - \Sigma_0 \propto d^m \quad (117)$$

with an exponent  $m$  of the order of  $-0.9$  for the mean curve in Fig. 12. The micromorphic model therefore can account for grain size effects with a saturation for too small grain sizes.

The dislocation density tensor  $\tilde{\Gamma} = \text{curl} \tilde{\chi}^p$  does not only impact the overall polycrystal behavior but also the way plastic deformation develops inside the grains. An example of the spreading of plastic deformation in a polycrystal depending on the grain size is shown in Fig. 13 for the 52–grain aggregate of Fig. 10(a). The shown maps are the contour plots of the field of equivalent plastic deformation  $p$ . At the onset of plastic deformation, plasticity starts in the same grains and at the same locations in  $100\mu\text{m}$ –grains as in  $1\mu\text{m}$ –grains, as shown by the pictures of Fig. 13(a) and (b). This is due to the fact that the same critical resolved shear stress is adopted for both grain sizes, corresponding to the same initial dislocation density. In contrast, at higher mean plastic strain levels, the strongly different values of the plastic microdeformation gradients lead to significantly different plastic strain fields. Two main features are evidenced by the Fig. 13(c) to (f). First, a tendency to strain localization in bands is observed for small grain sizes. The observed bands cross several grains whereas plastic strain is more diffuse at larger grain sizes. This fact was already observed in the

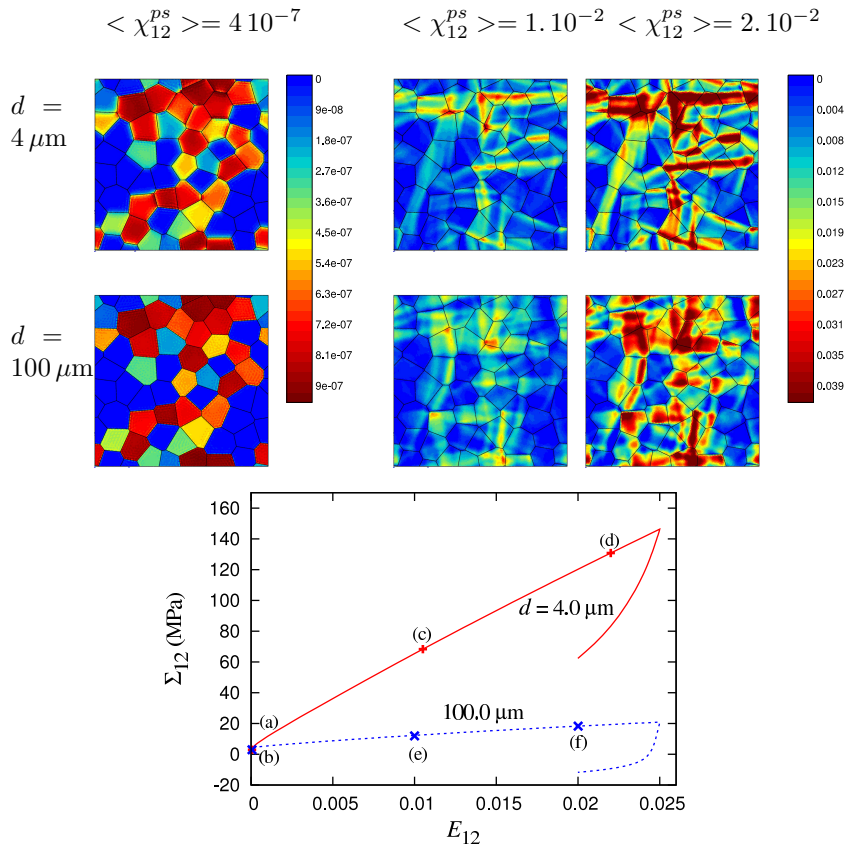


**Figure 13.** Contour plots of the accumulative plastic strain  $p$  for two grain sizes,  $d = 100$  and  $4 \mu\text{m}$ , and for three different mean values of the plastic strain :  $\langle \chi_{12}^{ps} \rangle \approx 0.$ ,  $\langle \chi_{12}^{ps} \rangle = 0.01$  and  $\langle \chi_{12}^{ps} \rangle = 0.02$ , obtained with the 55-grain aggregate of Fig. 10(c) under simple shear. (g) Macroscopic stress-strain response of the corresponding aggregate, letters indicating the loading steps for which the maps are shown.

simulations presented in Cordero et al. (2011, 2012). Second, a consequence of this localization is that some small grains are significantly less deformed than the larger ones.

## Bibliography

- E.C. Aifantis. On the microstructural origin of certain inelastic models. *Journal of Engineering Materials and Technology*, 106:326–330, 1984.
- J. Altenbach, H. Altenbach, and V.A. Eremeyev. On generalized cosserat-type theories of plates and shells: a short review and bibliography. *Arch. Appl. Mech.*, 80:73–92, 2010.
- A. Anthoine. Second-order homogenisation of functionally graded materials. *Int. J. Solids Structures*, 47:1477–1489, 2010.
- O. Aslan, N. M. Cordero, A. Gaubert, and S. Forest. Micromorphic approach to single crystal plasticity and damage. *International Journal of Engineering Science*, 49:1311–1325, 2011.
- N. Auffray, R. Bouchet, and Y. Bréchet. Derivation of anisotropic matrix for bi-dimensional strain-gradient elasticity behavior. *International Journal of Solids and Structures*, 46:440–454, 2009.
- N. Auffray, R. Bouchet, and Y. Bréchet. Strain gradient elastic homogenization of bidimensional cellular media. *International Journal of Solids and Structures*, 47:1698–1710, 2010.
- V.P. Bennett and D.L. McDowell. Crack tip displacements of microstructurally small surface cracks in single phase ductile polycrystals. *Engineering Fracture Mechanics*, 70(2):185–207, 2003.
- D. Besdo. Towards a Cosserat-theory describing motion of an originally rectangular structure of blocks. *Arch. Appl. Mech.*, 80:25–45, 2010.
- J. Besson, G. Cailletaud, J.-L. Chaboche, S. Forest, and M. Blétry. *Non-Linear Mechanics of Materials*. Series: Solid Mechanics and Its Applications, Vol. 167, Springer, ISBN: 978-90-481-3355-0, 433 p., 2009.
- C. Boutin. Microstructural effects in elastic composites. *Int. J. Solids Structures*, 33:1023–1051, 1996.
- F. Bouyge, I. Jasiuk, and M. Ostoja-Starzewski. A micromechanically based couple-stress model of an elastic two-phase composite. *Int. J. Solids Structures*, 38:1721–1735, 2001.
- F. Bouyge, I. Jasiuk, S. Boccara, and M. Ostoja-Starzewski. A micromechanically based couple-stress model of an elastic orthotropic two-phase composite. *European Journal of Mechanics A/solids*, 21:465–481, 2002.
- H. Chen, X. Liu, G. Hu, and H. Yuan. Identification of material parameters of micropolar theory for composites by homogenization method. *Computational Materials Science*, 46:733–737, 2009.
- N. M. Cordero, S. Forest, E. P. Busso, S. Berbenni, and M. Cherkaoui. Grain size effect in generalized continuum crystal plasticity. In I. R. Ionescu, S. Bouvier, O. Cazacu, and P. Franciosi, editors, *Plasticity of crystalline materials*, pages 101–122. ISTE-Wiley, 2011.

- N. M. Cordero, S. Forest, E. P. Busso, S. Berbenni, and M. Cherkaoui. Grain size effects on plastic strain and dislocation density tensor fields in metal polycrystals. *Computational Materials Science*, 52:7–13, 2012.
- N.M. Cordero, A. Gaubert, S. Forest, E. Busso, F. Gallerneau, and S. Kruch. Size effects in generalised continuum crystal plasticity for two-phase laminates. *Journal of the Mechanics and Physics of Solids*, 58:1963–1994, 2010.
- T. Dillard, S. Forest, and P. Ienny. Micromorphic continuum modelling of the deformation and fracture behaviour of nickel foams. *European Journal of Mechanics A/Solids*, 25:526–549, 2006.
- K. Enakoutsa and J.B. Leblond. Numerical implementation and assessment of the glpd micromorphic model of ductile rupture. *European Journal of Mechanics A/solids*, 28:445–460, 2009.
- A.C. Eringen. Theory of thermo-microstretch elastic solids. *Int. J. Engng Sci.*, 28:1291–1301, 1990.
- A.C. Eringen. *Microcontinuum field theories*. Springer, New York, 1999.
- A.C. Eringen and E.S. Suhubi. Nonlinear theory of simple microelastic solids. *Int. J. Engng Sci.*, 2:189–203, 389–404, 1964.
- F. Feyel. A multilevel finite element method (FE<sup>2</sup>) to describe the response of highly non-linear structures using generalized continua. *Comp. Meth. Appl. Mech. Engng*, 192:3233–3244, 2003.
- S. Forest. The micromorphic approach for gradient elasticity, viscoplasticity and damage. *ASCE Journal of Engineering Mechanics*, 135:117–131, 2009.
- S. Forest. Mechanics of generalized continua : Construction by homogenization. *Journal de Physique IV*, 8:Pr4–39–48, 1998.
- S. Forest. Homogenization methods and the mechanics of generalized continua—Part 2. *Theoretical and Applied Mechanics*, 28–29:113–143, 2002.
- S. Forest. Aufbau und Identifikation von Stoffgleichungen für höhere Kontinua mittels Homogenisierungsmethoden. *Technische Mechanik*, Band 19, Heft 4:297–306, 1999.
- S. Forest. Cosserat media. In K.H.J. Buschow, R.W. Cahn, M.C. Flemings, B. Ilshner, E.J. Kramer, and S. Mahajan, editors, *Encyclopedia of Materials : Science and Technology*, pages 1715–1718. Elsevier, 2001.
- S. Forest and A. Bertram. Formulations of strain gradient plasticity. In H. Altenbach, G. A. Maugin, and V. Erofeev, editors, *Mechanics of Generalized Continua*, pages 137–150. Advanced Structured Materials vol. 7, Springer, 2011.
- S. Forest and K. Sab. Cosserat overall modeling of heterogeneous materials. *Mechanics Research Communications*, 25(4):449–454, 1998.

- S. Forest and R. Sievert. Elastoviscoplastic constitutive frameworks for generalized continua. *Acta Mechanica*, 160:71–111, 2003.
- S. Forest and R. Sievert. Nonlinear microstrain theories. *International Journal of Solids and Structures*, 43:7224–7245, 2006.
- S. Forest and D. K. Trinh. Generalized continua and non-homogeneous boundary conditions in homogenization methods. *ZAMM*, 91:90–109, 2011.
- S. Forest, F. Pradel, and K. Sab. Asymptotic analysis of heterogeneous Cosserat media. *International Journal of Solids and Structures*, 38:4585–4608, 2001.
- M.G.D. Geers, V.G. Kouznetsova, and W.A.M Brekelmans. Gradient-enhanced computational homogenization for the micro-macro scale transition. *Journal de Physique IV*, 11:Pr5–145–152, 2001.
- P. Germain. The method of virtual power in continuum mechanics. part 2 : Microstructure. *SIAM J. Appl. Math.*, 25:556–575, 1973.
- J.D. Goddard. *Mathematical models of granular matter*, ed. by P. Mariano, G. Capriz, and P. Giovine, chapter From Granular Matter to Generalized Continuum, pages 1–20. vol. 1937 of Lecture Notes in Mathematics, Springer, Berlin, 2008.
- M. Gologanu, J. B. Leblond, and J. Devaux. *Continuum micromechanics*, volume 377, chapter Recent extensions of Gurson’s model for porous ductile metals, pages 61–130. Springer Verlag, CISM Courses and Lectures No. 377, 1997.
- M.A. Goodman and S.C. Cowin. A continuum theory for granular materials. *Arch. Rational Mech. and Anal.*, 44:249–266, 1972.
- P. Grammenoudis and Ch. Tsakmakis. Micromorphic continuum Part I: Strain and stress tensors and their associated rates. *International Journal of Non-Linear Mechanics*, 44:943–956, 2009.
- P. Grammenoudis, Ch. Tsakmakis, and D. Hofer. Micromorphic continuum Part II: Finite deformation plasticity coupled with damage. *International Journal of Non-Linear Mechanics*, 44:957–974, 2009.
- C.B. Hirschberger, E. Kuhl, and P. Steinmann. On deformational and configurational mechanics of micromorphic hyperelasticity - theory and computation. *Computer Methods in Applied Mechanics and Engineering*, 196:4027–4044, 2007.
- R. Jänicke and Diebels. A numerical homogenisation strategy for micromorphic continua. *Nuovo Cimento della Societa Italiana di Fisica C-Geophysics and Space Physics*, 32:121–132, 2009.
- R. Jänicke, S. Diebels, H.-G. Sehlhorst, and A. Düster. Two-scale modelling of micromorphic continua. *Continuum Mechanics and Thermodynamics*, 21:297–315, 2009.

- C.B. Kafadar and A.C. Eringen. Micropolar media: I the classical theory. *Int. J. Engng Sci.*, 9:271–305, 1971.
- T. Kanit, S. Forest, I. Galliet, V. Mounoury, and D. Jeulin. Determination of the size of the representative volume element for random composites : statistical and numerical approach. *International Journal of Solids and Structures*, 40:3647–3679, 2003.
- N. Kirchner and P. Steinmann. A unifying treatise on variational principles for gradient and micromorphic continua. *Philosophical Magazine*, 85: 3875–3895, 2005.
- V. G. Kouznetsova, M. G. D. Geers, and W. A. M. Brekelmans. Multi-scale constitutive modelling of heterogeneous materials with a gradient-enhanced computational homogenization scheme. *Int. J. Numer. Meth. Engng*, 54:1235–1260, 2002.
- V. G. Kouznetsova, M. G. D. Geers, and W. A. M. Brekelmans. Multi-scale second-order computational homogenization of multi-phase materials : A nested finite element solution strategy. *Computer Methods in Applied Mechanics and Engineering*, 193:5525–5550, 2004.
- S. Kruch and S. Forest. Computation of coarse grain structures using a homogeneous equivalent medium. *Journal de Physique IV*, 8:Pr8–197–205, 1998.
- M. Lazar and G.A. Maugin. On microcontinuum field theories: the eshelby stress tensor and incompatibility conditions. *Philosophical Magazine*, 87: 3853–3870, 2007.
- X. Liu and G. Hu. Inclusion problem of microstretch continuum. *International Journal of Engineering Science*, 42:849–860, 2003.
- J. Mandel. Equations constitutives et directeurs dans les milieux plastiques et viscoplastiques. *Int. J. Solids Structures*, 9:725–740, 1973.
- G.A. Maugin. Internal variables and dissipative structures. *J. Non-Equilib. Thermodyn.*, 15:173–192, 1990.
- R.D. Mindlin. Micro-structure in linear elasticity. *Arch. Rat. Mech. Anal.*, 16:51–78, 1964.
- R.D. Mindlin. Second gradient of strain and surface-tension in linear elasticity. *Int. J. Solids Structures*, 1:417–438, 1965.
- M. Ostoja-Starzewski, S. D. Boccara, and I. Jasiuk. Couple-stress moduli and characteristic length of two-phase composite. *Mechanics Research Communication*, 26:387–396, 1999.
- R.A. Regueiro. On finite strain micromorphic elastoplasticity. *International Journal of Solids and Structures*, 47:786–800, 2010.
- G. Salerno and F. de Felice. Continuum modeling of periodic brickwork. *International Journal of Solids and Structures*, 46:1251–1267, 2009.

- E. Sanchez-Palencia. Comportement local et macroscopique d'un type de milieux physiques hétérogènes. *International Journal of Engineering Science*, 12:331–351, 1974.
- V. Sansalone, P. Trovalusci, and F. Cleri. Multiscale modeling of materials by a multifield approach : microscopic stress and strain distribution in fiber-matrix composites. *Acta Materialia*, 54:3485–3492, 2006.
- C. Sansour. A unified concept of elastic–viscoplastic Cosserat and micromorphic continua. *Journal de Physique IV*, 8:Pr8–341–348, 1998a.
- C. Sansour. A theory of the elastic–viscoplastic cosserat continuum. *Archives of Mechanics*, 50:577–597, 1998b.
- C. Sansour, S. Skatulla, and H. Zbib. A formulation for the micromorphic continuum at finite inelastic strains. *Int. J. Solids Structures*, 47:1546–1554, 2010.
- H. Steeb and S. Diebels. A thermodynamic–consistent model describing growth and remodeling phenomena. *Computational Materials Science*, 28:597–607, 2003.
- P. Trovalusci and R. Masiani. Non-linear micropolar and classical continua for anisotropic discontinuous materials. *International Journal of Solids and Structures*, 40:1281–1297, 2003.
- C. Truesdell and W. Noll. *The non-linear field theories of mechanics*. Handbuch der Physik, edited by S. Flügge, reedition Springer Verlag 2004, 1965.
- C.A. Truesdell and R.A. Toupin. *Handbuch der Physik*, S. Flügge, editor, vol. 3, chapter The classical field theories, pages 226–793. Springer verlag, Berlin, 1960.
- F. Xun, G. Hu, and Z. Huang. Size–dependence of overall in–plane plasticity for fiber composites. *International Journal of Solids and Structures*, 41:4713–4730, 2004.
- X. Yuan, Y. Tomita, and T. Andou. A micromechanical approach of non-local modeling for media with periodic microstructures. *Mechanics Research Communications*, 35:126–133, 2008.